Expanded Analysis of Hot Isostatic Pressed Iodine-Loaded Silver-Exchanged Mordenite

Fuel Cycle Research & Development

Prepared for U.S. Department of Energy Separations and Waste Forms R. T. Jubin, S. H. Bruffey, and K. K. Patton Oak Ridge National Laboratory September 2014 FCRD-SWF-2014-000278 ORNL/LTR-2014/476



DISCLAIMER

This information was prepared as an account of work sponsored by an agency of the U.S. Government. Neither the U.S. Government nor any agency thereof, nor any of their employees, makes any warranty, expressed or implied, or assumes any legal liability or responsibility for the accuracy, completeness, or usefulness, of any information, apparatus, product, or process disclosed, or represents that its use would not infringe privately owned rights. References herein to any specific commercial product, process, or service by trade name, trade mark, manufacturer, or otherwise, does not necessarily constitute or imply its endorsement, recommendation, or favoring by the U.S. Government or any agency thereof. The views and opinions of authors expressed herein do not necessarily state or reflect those of the U.S. Government or any agency thereof.

SUMMARY

Reduced silver-exchanged mordenite (Ag⁰Z) is being evaluated as a potential material to control the release of radioactive iodine that is released during the reprocessing of used nuclear fuel into the plant off-gas streams. The purpose of this study was to determine if hot pressing could directly convert this iodine loaded sorbent into a waste form suitable for long-term disposition. The minimal pretreatment required for production of pressed pellets makes hot pressing a technically and economically desirable process.

Initial scoping studies utilized hot uniaxial pressing (HUPing) to prepare samples of non-iodine-loaded reduced silver exchanged mordenite (Ag^0Z). The resulting samples were very fragile due to the low pressure (~ 28 MPa) used. It was recommended that hot isostatic pressing (HIPing), performed at higher temperatures and pressures, be investigated.

HIPing was carried out in two phases, with a third and final phase currently underway. Phase I evaluated the effects of pressure and temperature conditions on the manufacture of a pressed sample. The base material was an engineered form of silver zeolite. Six samples of Ag^0Z and two samples of I- Ag^0Z were pressed. It was found that HIPing produced a pressed pellet of high density. Analysis of each pressed pellet by scanning electron microscopy-energy dispersive spectrophotometry (SEM-EDS) and X-ray diffraction (XRD) demonstrated that under the conditions used for pressing, the majority of the material transforms into an amorphous structure. The only crystalline phase observed in the pressed Ag^0Z material was SiO_2 . For the samples loaded with iodine (I- Ag^0Z) iodine was present as AgI clusters at low temperatures, and transformed into $AgIO_4$ at high temperatures. Surface mapping and EDS demonstrate segregation between silver iodide phases and silicon dioxide phases.

Based on the results of the Phase I study, an expanded test matrix was developed to examine the effects of multiple source materials, compositional variations, and an expanded temperature range. Each sample was analyzed with the approach used in Phase I. In all cases, there is nothing in the SEM or XRD analyses that indicates creation of any AgI-containing silicon phase, with the samples being found to be largely amorphous. Phase III of this study has been initiated and is the final phase of scoping tests. It will expand upon the test matrix completed in Phase II and will examine the durability of the pressed pellets through product consistency testing (PCT) studies. Transformation of the component material into a well-characterized iodine-containing mineral phase would be desirable. This would limit the additional experimental testing and modeling required to determine the long-term stability of the pressed pellet, as much of that information has already been learned for several common iodine-containing minerals. However, this is not an absolute requirement, especially if pellets produced by hot isostatic pressing can be demonstrated through initial PCT studies to retain iodine well despite their amorphous composition.

ACKNOWLEDGEMENTS

We would like to acknowledge Clint Ausmus for his assistance in cross-sectioning and mounting the pressed samples, and Roberta Meisner and Shawn Reeves for their analysis of the pressed samples by XRD and SEM-EDS.

CONTENTS

SU	UMMARY	iii
AC	CKNOWLEDGEMENTS	iv
FIC	IGURES	vi
TA	ABLES	viii
AC	CRONYMS	ix
1.	INTRODUCTION	1
2.	BACKGROUND	1
3.	MATERIALS	2
4.	HOT UNIAXIAL PRESSING	2
5.	HOT ISOSTATIC PRESSING	6
	5.1 Phase I Pressing and Analysis	6
	5.2 Phase II Pressing and Analysis	21 21
6.	DISCUSSION	28
7.	REFERENCES	29
Ap	ppendix A Cross Sections of Phase I and II Samples	30
Аp	ppendix B Elemental Maps of Pressed Samples	33
Αp	ppendix C XRD Patterns of Phase II Samples	37

FIGURES

Fig. 1. Crushed Ag ⁰ Z used in HUP testing.	3
Fig. 2. Hot uniaxial press and furnace used in initial testing for Ag ⁰ Z pressing	3
Fig. 3. HUPed compacts formed from pelletized (l) and crushed (r) engineered Ag ⁰ Z	4
Fig. 4. Side view of HUPed compacts formed from pelletized (l) and crushed (r) engineered Ag^0Z .	4
Fig. 5. Cross section of HUPed compact formed from engineered Ag ⁰ Z.	5
Fig. 6. Crushed HUPed compact formed from engineered Ag ⁰ Z.	5
Fig. 7. End of I-Ag ⁰ Z loaded capsule 1-8.	7
Fig. 8. Side view of I-Ag ⁰ Z loaded capsule 1-8.	8
Fig. 9. HIPed capsule 1-8 containing I-Ag ⁰ Z.	8
Fig. 10. HIPed capsule 1-8 containing I-Ag ⁰ Z.	9
Fig. 11. HIPed capsule 1-7 containing I-Ag ⁰ Z.	9
Fig. 12. Cross section of HIPed sample 1-2 (700°C and 100 MPa)	11
Fig. 13. Cross section of HIPed sample 1-3 (700°C and 175 MPa)	11
Fig. 14. Cross section of HIPed sample 1-6 (crushed Ag ⁰ Z, 700°C and 100 MPa)	11
Fig. 15. Cross section of HIPed sample 1-8 containing I-Ag ⁰ Z (700°C and 175 MPa)	12
Fig. 16. XRD pattern of HIPed sample 1-4 (525°C and 100 MPa).	13
Fig. 17. Combined XRD patterns for HIPed samples 1-2 (700°C and 100 MPa), 1-3 (700°C and 175 MPa), 1-5 (850°C and 100 MPa), and 1-6 (700°C and 100 MPa)	14
Fig. 18. XRD pattern of HIPed sample 1-7 containing I-Ag ⁰ Z (525°C and 175 MPa)	15
Fig. 19. XRD pattern of HIPed sample 1-8 containing I-Ag ⁰ Z (700°C and 175 MPa)	16
Fig. 20. Sample surfaces 1-2, 1-3, 1-5, 1-6, 1-7, and 1-8 at 500× magnification.	17
Fig. 21. Clusters of silver and iodine observed in samples 1-6, 1-7, and 1-8 at 5000× magnification.	17
Fig. 22. Elemental maps of HIPed sample surface 1-5 (Ag ⁰ Z, 850°C, 100 MPa)	18
Fig. 23. Elemental maps of HIPed sample surface 1-7 (I-Ag ⁰ Z, 525°C, 175 MPa)	18
Fig. 24. SEM-EDS of sample 1-5: a) EDS analysis of a silver cluster, b) EDS analysis of the area adjacent to the cluster.	19
Fig. 25. SEM-EDS of sample 1-8: a) EDS of a silicon structure, b) EDS of AgI clusters observed adjacent to the silicon structure.	20
Fig. 26. Cross section of sample 2-13 (engineered $Ag^0Z + AgI\ 3:1;\ 900^{\circ}C$ and $100\ MPa$)	22
Fig. 27. Cross section of sample 2-7 (NaZ + AgI 3:1; 700°C and 300 MPa)	23
Fig. 28. Cross section of sample 2-11 (NaZ + AgI 3:1; 900°C and 100 MPa)	23
Fig. 29. XRD pattern of HIPed samples 2-1, 2-2, and 2-3 (NaZ powder + AgI 3:1; 525, 700, and 900°C respectively)	25

Fig. 30. Surfaces of sample 2-2 (a), sample 2-6 (b), sample 2-7 (c), and sample 2-24 (d) at 400× magnification (pressing conditions and sample compositions found in Table 7)	26
Fig. 31. Surface of sample 2-13 (containing engineered Ag ⁰ Z) at 2000× magnification	27
Fig. 32. Elemental maps for sample 2-1 at 5000× magnification.	27
Fig. 33. SEM-EDS of sample 2-3: a) EDS of a silicon structure, b) EDS of AgI clusters observed adjacent to the silicon structure.	28
Fig. A-1. Cross section of sample 1-5 (850°C, 100 MPa).	30
Fig. A-2. Cross section of sample 1-7 (525°C, 175 MPa).	30
Fig. A-3. Cross section of sample 2-2 (700°C, 175 MPa).	31
Fig. A-4. Cross section of sample 2-5 (900°C, 175 MPa).	31
Fig. A-5. Cross section of sample 2-6 (700°C, 300 MPa).	32
Fig. A-6. Cross section of sample 2-13 (900°C, 175 MPa).	32
Fig. B-1. Elemental maps for sample 2-1 at ≈500× magnification.	33
Fig. B-2. Elemental maps for sample 1-3 at ≈500× magnification.	33
Fig. B-3. Elemental maps for sample 1-4 at ≈500× magnification.	34
Fig. B-4. Elemental maps of sample 1-8 at 5000× magnification.	34
Fig. B-5. Elemental maps of sample 2-7 at 50000× magnification.	35
Fig. B-6. Elemental maps of sample 2-11 at 5000× magnification.	35
Fig. B-7. Elemental maps of sample 2-12 at 5000× magnification.	36
Fig. C-1. XRD pattern of HIPed samples 2-5, 2-6, and 2-7 (pressing conditions and sample composition found in Table 7)	37
Fig. C-2. XRD pattern of HIPed samples 2-11, 2-12, and 2-13 (pressing conditions and sample composition found in Table 7)	38
Fig. C-3. XRD pattern of HIPed samples 2-21 and 2-24 (pressing conditions and sample composition found in Table 7).	38

TABLES

Table 1. Physical property data on HUPed Ag ⁰ Z compacts	6
Table 2. Phase I test matrix	<i>6</i>
Table 3. Parameter explored in Phase I testing	
Table 4. Density of HIPed Phase I samples	
Table 5. Phase II test matrix	21
Table 6. Parameter explored in Phase II testing	22
Table 7. Density of HIPed Phase II samples	24

ACRONYMS

Ag⁰Z Reduced silver-exchanged mordenite

ANL Argonne National Laboratory

HIPing Hot isostatic pressing HUPing Hot uniaxial pressing

I-Ag⁰Z Iodine-loaded reduced silver-exchanged mordenite

INL Idaho National Laboratory

ORNL Oak Ridge National Laboratory

PCT Product consistency test

SEM Scanning electron microscopy

SEM-EDS Scanning electron microscopy—energy dispersive spectrophotometry

XRD X-ray diffraction

SEPARATIONS AND WASTE FORMS CAMPAIGN/FUEL CYCLE RESEARCH AND DEVELOPMENT: EXPANDED ANALYSIS OF HOT ISOSTATIC PRESSED IODINE-LOADED SILVER-EXCHANGED MORDENITE

1. INTRODUCTION

Reduced silver-exchanged mordenite (Ag^0Z) is being evaluated as a potential material to control the release of radioactive iodine during the reprocessing of used nuclear fuel into the plant off-gas streams. The objective of this report is to provide a brief synopsis of the results collected in FY 2014 on the potential use of hot uniaxial pressing (HUPing) or hot isostatic pressing (HIPing) to convert iodine-loaded reduced silver-exchanged mordenite (I- Ag^0Z) into a suitable waste form. The following sections provide a brief background on the use of the HUPing and HIPing processes and their use in waste form production, an overview of the materials and methods used, the results of the initial HUPing scoping studies conducted with non-iodine-loaded reduced silver-exchanged mordenite (Ag^0Z), and the results of each phase of the HIPing study.

Transformation of the component material into a well-characterized iodine-containing mineral phase would be desirable. This would limit the additional experimental testing and modeling required to determine the long-term stability of the pressed pellet, as much of that information has already been learned for several common iodine-containing minerals.

2. BACKGROUND

Determination of pressing conditions for this testing was guided by a literature review of similar studies. The limited amount of information available indicates that this is a novel approach to iodine waste form production.

In the late 1970s and early 1980s, Idaho National Laboratory (INL) examined the technical feasibility of immobilizing krypton-85 in a HIPed zeolite structure. No additional binder material was added, and the zeolite was sintered at 700°C and 100 MPa for 2 to 4 hr. Loading of 30 to 60 m³ of krypton per cubic meter of solid was possible. The product was amorphous, and krypton leakages were very low at temperatures up to 750°C.

Work at Argonne National Laboratory (ANL) and INL in the 1990's focused on waste form development for the E-chem process. This work utilized a glass frit and zeolite loaded with fission products. This mixture was HIPed at temperatures of 700 to 750°C and pressures of 41 to 172 MPa. The zeolites included 3A, 4A, and 5A framework types and contained 21 wt% salt mixed with up to 45% glass frit. A pressureless version involved heating the material to 925°C.

In 2005, the National Nuclear Laboratory in the United Kingdom demonstrated HIPing of A and X zeolites at 900°C, converting them to a sodalite.⁴

In Japan, work was conducted in 2007 on the sintering of silver nitrate–impregnated silica gel (AgS).⁵ The particle size was 45 μ m, and no additional material was added. The material was sintered at 700°C and 100 MPa for 3 hr. Silver nitrate–impregnated alumina (AgA) was also sintered at 850°C and 175 MPa for 3 hr.

After review, the pressing conditions selected ranged from 525 to 1100°C and 100–300 MPa and are discussed in greater detail in the next section. The upper limits of both the pressure and temperature ranges selected are higher than previously seen in the literature and will demonstrate whether such conditions result in an improvement in the characteristics of the produced waste pellet. Two types of hot pressing were evaluated in this study. The first, HUPing, exerts pressure upon the sample along a single axis. The second, HIPing, exerts pressure on the sample uniformly from all directions. Oak Ridge National Laboratory (ORNL) possesses HUPing capabilities but contracts with a commercial vendor for HIPing.

3. MATERIALS

Sodium iodide powder (99.9% pure, metals basis) and silver iodide powder (99.999% pure, metals basis) were purchased from Alfa Aesar. Synthetic sodium mordenite powder was manufactured by Wako Chemicals. Silver mordenite powder was produced at ORNL by ion exchange of the sodium mordenite powder.

Engineered, pelletized silver mordenite (Zeolon 900) was obtained from Molecular Products (Ionex-Type Ag 900 E16). It contained 9.5% silver by weight and has 1/16 in. pellet diameter. Prior to use in this experiment, the material underwent a hydrogen reduction to reduce silver incorporated in the material, thus forming Ag^0Z . The reduction was performed by drying a deep bed of AgZ at $270^{\circ}C$ with a low flow of argon, then reducing the material for 10 days at $270^{\circ}C$ with a gas mixture of $4\%H_2/96\%$ N_2 .

4. HOT UNIAXIAL PRESSING

An initial attempt assessed the use of HUPing to prepare two pressed samples of non-iodine-loaded Ag⁰Z and evaluated the resulting product. The first pressed sample consisted of the engineered pelletized form produced by the manufacturer, and the second sample consisted of the same material that had been crushed using a mortar and pestle. No sieving was performed on the crushed material prior to pressing, as shown in Fig. 1. The cover gas was argon at 10 in. of Hg, and the pressing was conducted at ~4000 psi (~27.5 MPa) at 750°C for 1 hr. The furnace and press are shown in Fig. 2. Figures 3 and 4 show the resulting compacts from intact Ag⁰Z pellets and from crushed Ag⁰Z. Figure 5 shows the cross section of the compact pressed from the intact form of engineered Ag⁰Z.

An attempt was made to determine the crush strength of the resulting compact by placing one-half of the sectioned compact between two gauge blocks. As soon as the handle of the gauge was moved, the pellet fractured. No recording was made of the pressure. The fractured compact is shown in Fig. 6.

The properties of the HUPed pellets are shown in Table 1. Minimal weight loss (<50 mg) was observed for these compacts, but the Ag⁰Z contained no iodine. Weight loss during the HUPing process may result from either water loss from the hydrated mordenite or from the volatilization of small amounts of iodine, if present. Minimizing the loss of iodine is a key component when considering hot pressing as a viable process because the melting point of AgI (the expected chemical form of iodine in the waste form) is

558°C, whereas the processes may be conducted as high as 1100°C. The bulk volume of the Ag^0Z was reduced in both samples by ~50% after HUPing.



Fig. 1. Crushed Ag⁰Z used in HUP testing.



Fig. 2. Hot uniaxial press and furnace used in initial testing for Ag⁰Z pressing.



Fig. 3. HUPed compacts formed from pelletized (l) and crushed (r) engineered Ag⁰Z.



Fig. 4. Side view of HUPed compacts formed from pelletized (l) and crushed (r) engineered Ag⁰Z.



Fig. 5. Cross section of HUPed compact formed from engineered Ag⁰Z.



Fig. 6. Crushed HUPed compact formed from engineered Ag⁰Z.

·	1 1 0	
	Crushed Ag ⁰ Z	Pellet form Ag ⁰ Z
Diameter (in.)	0.506	0.510
Height (in.)	0.703	0.705
Final weight (g)	3.0150	3.0926
Density (g/cm ³)	1.29	1.30

Table 1. Physical property data on HUPed Ag⁰Z compacts

The pressures used in this HUPing were relatively low compared to the pressures used in previously reported HIPing of either krypton-85 loaded zeolite 5A, which was conducted at 700°C and 100 MPa for 2 to 4 hr, or several iodine waste forms that were pressed at temperatures ranging from 700 to 900°C and pressures from 100 to 175 MPa.

5. HOT ISOSTATIC PRESSING

To evaluate the benefits of higher pressures on waste form production, a contract was placed with a commercial vendor, American Isostatic Presses, Inc., to conduct HIPing. These tests were conducted in two phases. Phase 1 examined pressure and temperature variations on a single source material (engineered Ag⁰Z) that was pressed either as-received or loaded with iodine. Phase 2 was broader in scope, evaluating multiple source materials, compositional variations, and an expanded temperature range.

5.1 Phase I Pressing and Analysis

5.1.1 Sample Test Matrix

The sample matrix developed for Phase I of the HIPing tests is shown in Table 2. The initial temperature range of interest was 525 to 850°C and with a pressure of 100 or 175 MPa. The temperature ramp rate was approximately 10°C/min. Samples 2 through 5 of the matrix allowed the effects of pressure and temperature variations on capsule density to be determined. Samples 1-7 and 1-8, pressed I-Ag⁰Z, provided insight into the effects of iodine presence on pressing and whether there is any migration of iodine as a result of different temperatures involved in the pressing process. The parameters studied by use of the test matrix are shown in Table 3.

Sample ^a	Temperature (°C)	Pressure (MPa)	Time (hr)	Particle form
1-2	700	100	3	Intact Ag ⁰ Z
1-3	700	175	3	Intact Ag ⁰ Z
1-4	525	100	3	Intact Ag ⁰ Z
1-5	850	100	3	Intact Ag ⁰ Z
1-6	700	100	3	Crushed Ag ⁰ Z
1-7	525	175	3	Intact I-Ag ⁰ Z
1-8	700	175	3	Intact I-Ag ⁰ Z

Table 2. Phase I test matrix

^aSample 1-1 was not successfully encapsulated, preventing pressing

		•		
Set	Samples	Primary effect studied		
1 2, 3		HIP pressure		
2	2, 4, 5	HIP temperature		
3 2,6		Sizing		
4	3, 8	Presence of I		
5	7, 8	Temperature on Ag or I migration		

Table 3. Parameter explored in Phase I testing

The sample containers were constructed of 304 stainless steel tubing, and each contained approximately 5 g of Ag^0Z or I- Ag^0Z . The wall thickness was 0.020 in., the end caps were 0.010 in. thick, and the internal volume was estimated to be 6.5 cm³. The capsules were sealed using electron beam welding in a vacuum chamber. Figures 7 and 8 show a representative sample capsule prior to pressing. Figures 9, 10, and 11 show representative post-pressing samples.



Fig. 7. End of I-Ag⁰Z loaded capsule 1-8.



Fig. 8. Side view of I-Ag⁰Z loaded capsule 1-8.



Fig. 9. HIPed capsule 1-8 containing I-Ag⁰Z.



Fig. 10. HIPed capsule 1-8 containing I-Ag⁰Z.



Fig. 11. HIPed capsule 1-7 containing I-Ag⁰Z.

5.1.2 Analysis of Phase I Samples

The density of the resulting product in the pressed samples was determined from the volume of the crushed container by volume displacement using a graduated cylinder. The volume of the stainless steel used to form the capsule was assumed to be unaffected by the HIPing, and the volume of the stainless steel was calculated based on the weight of the stainless steel in each original capsule using a density of 8.03 g/cm³. Table 4 shows the resulting densities of the HIPed samples. The densities resulting from HIPing are significantly higher than those from the hot uniaxial pressing. There is a direct correlation between increased HIP pressure and increased HIP temperature, and increased density of the pressed capsule. There was no correlation between the density of the produced pellet and crushing of the sample prior to HIPing.

At 175 MPa the calculated density of the AgZ was 2.6-2.65 g/cm³. This is an increase in density of ~340% over the bulk density of the starting material (0.77 g/cm³). At 100 MPa the density was increased by ~275% with the one exception of the sample that was pressed at 850° C, which also achieved a density of ~ 2.6 g/cm³. This is a significant increase in sample density over previous HUPing tests in which the density was increased by only 170%.

Sample	Temperature (°C)	Pressure (MPa)	Time (hr)	Particle form	Density (g/cm ³)
1-2	700	100	3	Intact Ag ⁰ Z	2.12
1-3	700	175	3	Intact Ag ⁰ Z	2.65
1-4	525	100	3	Intact Ag ⁰ Z	1.95
1-5	850	100	3	Intact Ag ⁰ Z	2.62
1-6	700	100	3	Crushed Ag ⁰ Z	2.06
1-7	525	175	3	Intact I- Ag ⁰ Z	2.62
1-8	700	175	3	Intact I-Ag ⁰ Z	2.50

Table 4. Density of HIPed Phase I samples

Figures 12 and 13 show the cross sections for HIPed Ag⁰Z samples 1-2 and 1-3. These were both HIPed at 700°C but at different pressures. No obvious differences were observed at this resolution even though the density of sample 1-3 was higher. Figure 14 shows a cross section of capsule 1-6, which contained crushed Ag⁰Z. This was HIPed under the same conditions as capsule 1-2, which contained intact Ag⁰Z (Fig. 12). Figure 15 is a cross section of capsule 1-8, which contained I- Ag⁰Z. This capsule was HIPed under the same conditions as sample 1-3 (Fig. 13). This cross section shows a marked change in the color of the compressed material. The cross sections for sample 1-5 and sample 1-7 are found in Appendix A.



Fig. 12. Cross section of HIPed sample 1-2 (700°C and 100 MPa).



Fig. 13. Cross section of HIPed sample 1-3 (700°C and 175 MPa).



Fig. 14. Cross section of HIPed sample 1-6 (crushed Ag⁰Z, 700°C and 100 MPa).



Fig. 15. Cross section of HIPed sample 1-8 containing I-Ag⁰Z (700°C and 175 MPa).

The surface of each cross-sectioned sample was analyzed by X-ray diffraction (XRD) to determine the mineral phases present after HIPing. It was expected that mordenite, which is thermally unstable at the temperatures used during pressing, would transform to other phases or decompose during the process.⁶

In all samples, large amorphous peaks were present in the XRD patterns, as well as SiO_2 in the form of quartz or cristobalite. With the exception of sample 1-4 (pressed at the lowest combined pressure and temperature), no mordenite was observed to remain in the pressed samples. The XRD pattern for sample 1-4 is shown in Fig. 16 and demonstrates the presence of mordenite.

The XRD patterns for samples 1-2, 1-3, 1-5, and 1-6 are shown in Fig. 17. The strongest peak in these samples is quartz, with no other crystalline phases observed.

The XRD patterns for samples 1-7 and 1-8 are shown in Figs. 18 and 19, respectively. These samples each originally consisted of I-Ag⁰Z, and two resulting iodine phases, Ag(IO₄) and AgI, are observed in these samples. Sample 1-7, pressed at a lower temperature than sample 8 (525°C vs 700°C), appears to only contain iodine in the form of AgI. Iodine would be expected to be retained in silver mordenite prior to any HIPing as AgI. Upon pressing at higher temperatures such as tested in sample 1-8, the silver-iodine complex appears to transform into silver iodate (AgIO₄).

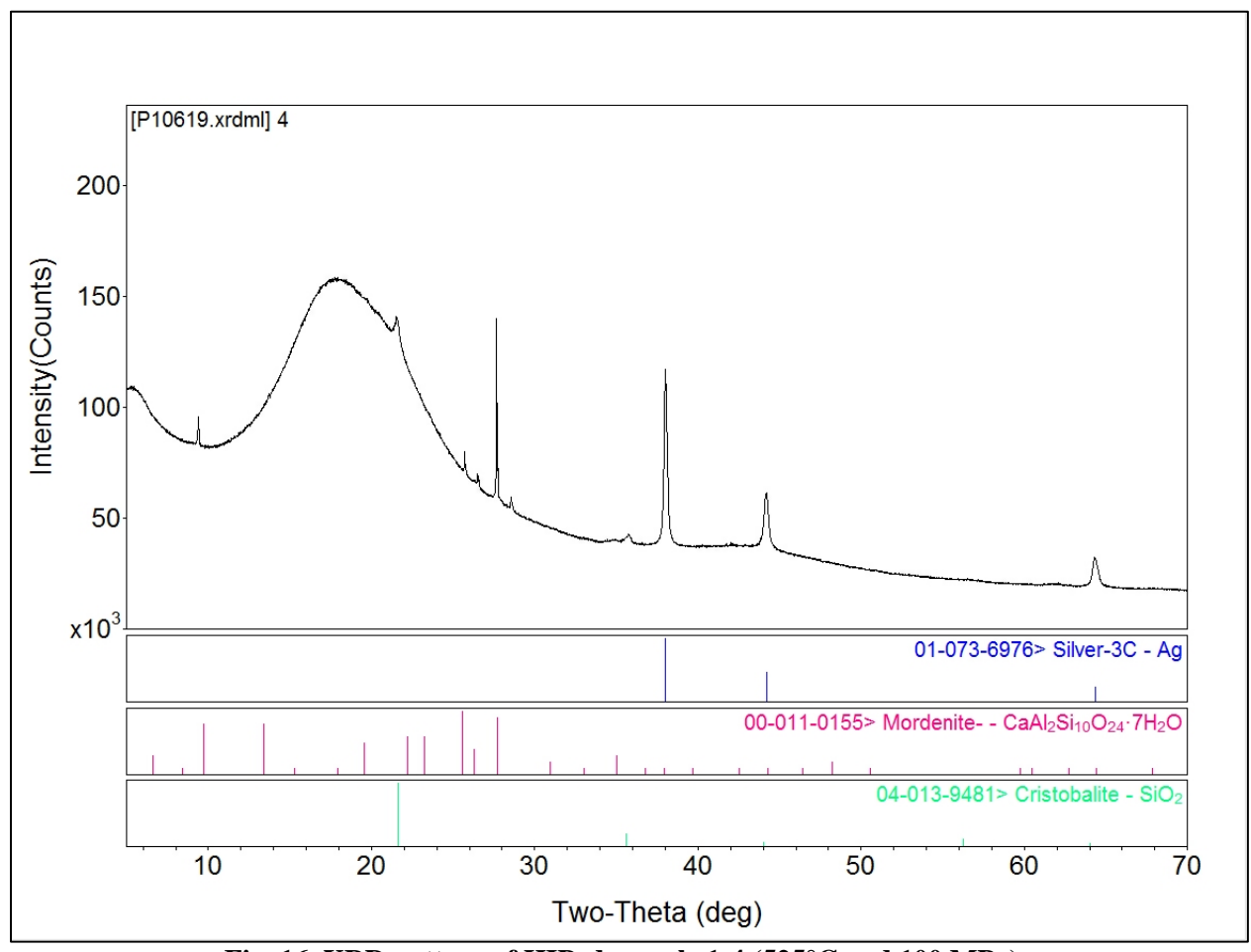


Fig. 16. XRD pattern of HIPed sample 1-4 (525°C and 100 MPa).

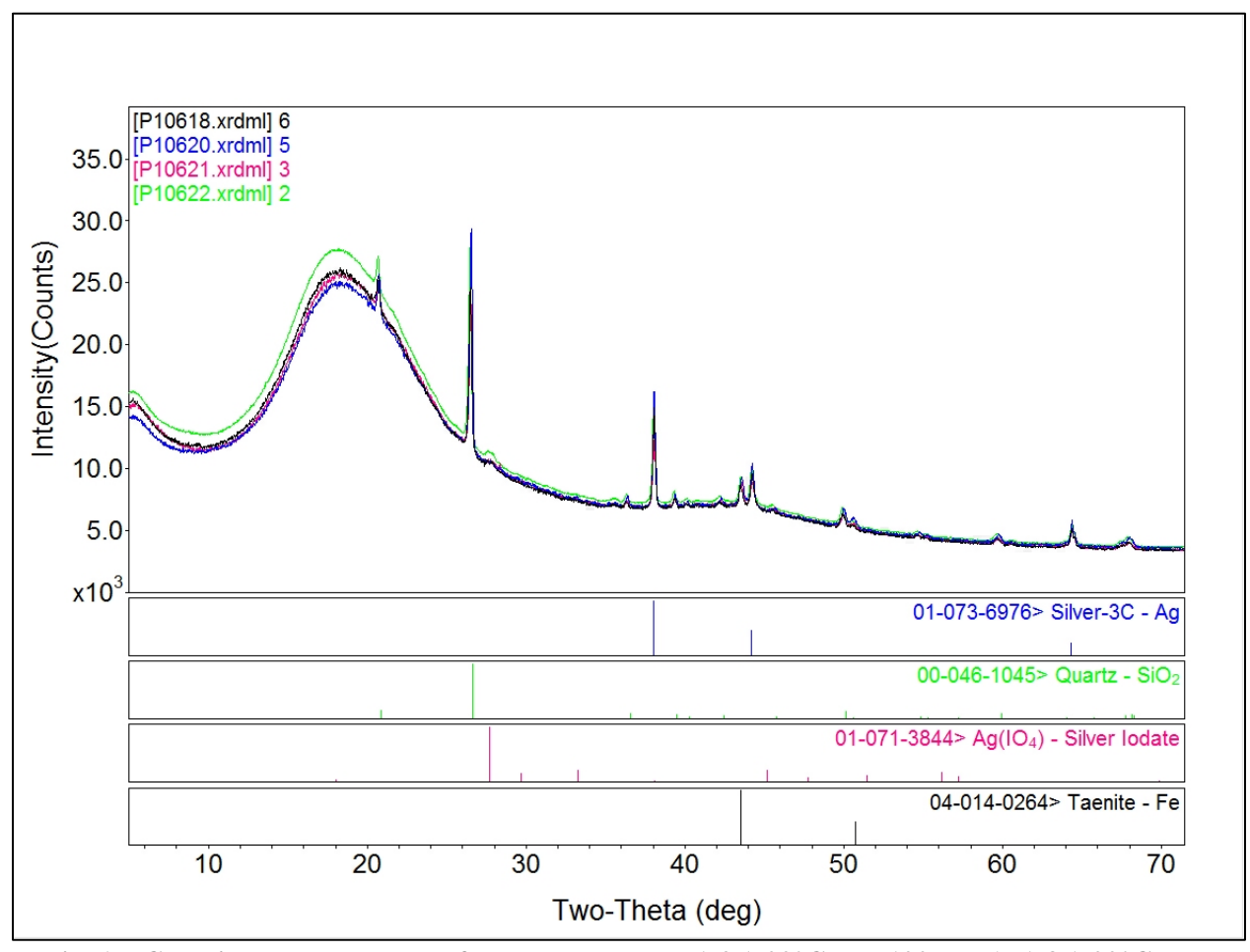


Fig. 17. Combined XRD patterns for HIPed samples 1-2 (700° C and 100 MPa), 1-3 (700° C and 175 MPa), 1-5 (850° C and 100 MPa), and 1-6 (700° C and 100 MPa).

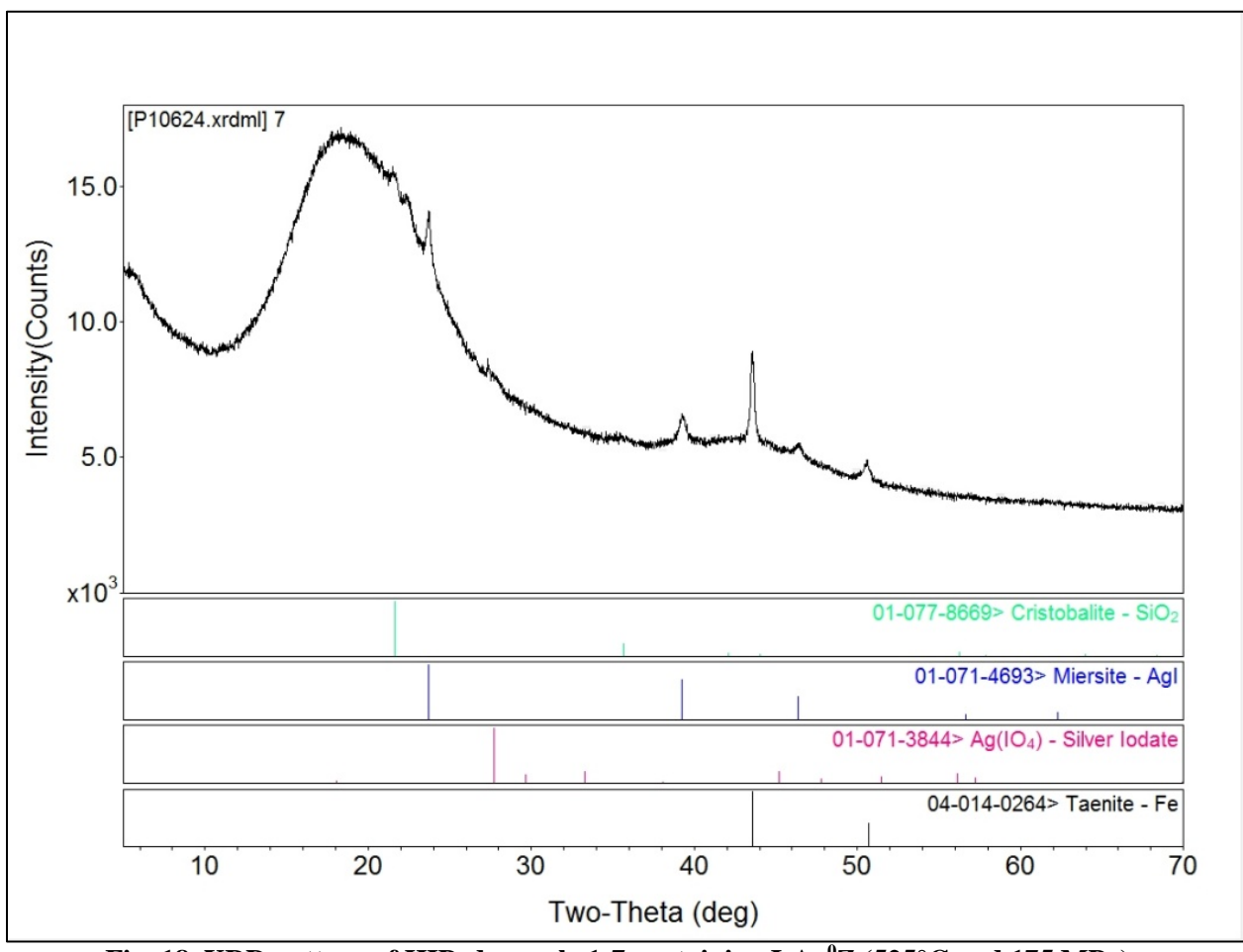


Fig. 18. XRD pattern of HIPed sample 1-7 containing I-Ag⁰Z (525°C and 175 MPa).

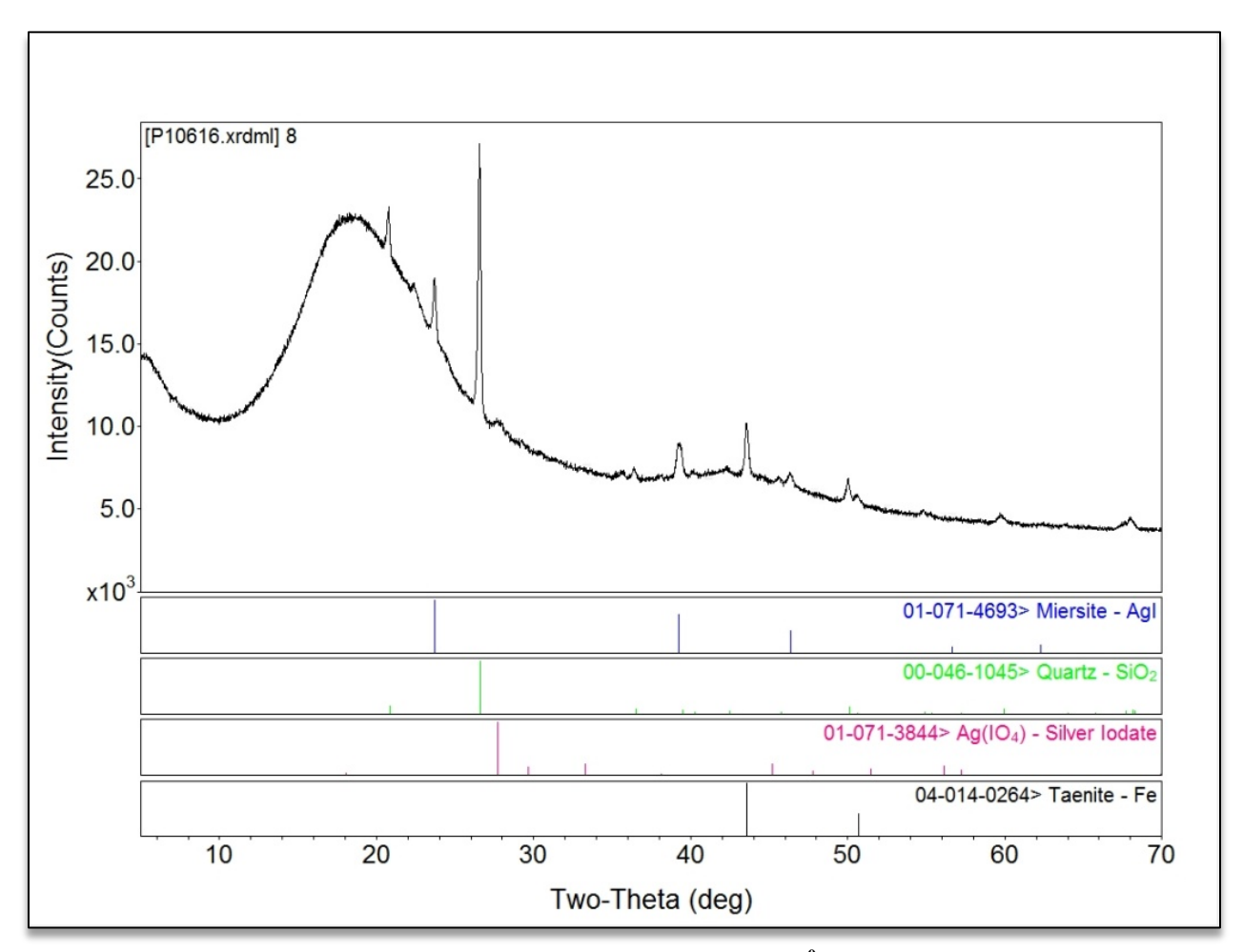


Fig. 19. XRD pattern of HIPed sample 1-8 containing I-Ag⁰Z (700°C and 175 MPa).

To conclude the analysis of the Phase I samples, the surface of each sample was examined by scanning electron microscopy (SEM) on a Hitachi S-4800. This instrument utilizes an electron beam accelerated at 500V to 30kV and possesses both a secondary electron detector and a backscattering electron detector. First, each sample was examined at low magnification, revealing the presence of a significant amount of surface pitting (Fig. 20). While surface pitting can come about during the sample mounting and polishing process, it is possible that the pits are an artifact of the HIPing itself. Each sample was also examined at higher magnifications. For samples 1-5 through 1-8, cluster-like structures were observed (samples 1-6, 1-7, and 1-8 are shown in Fig. 21). This heterogeneity was examined further by the collection of elemental maps.

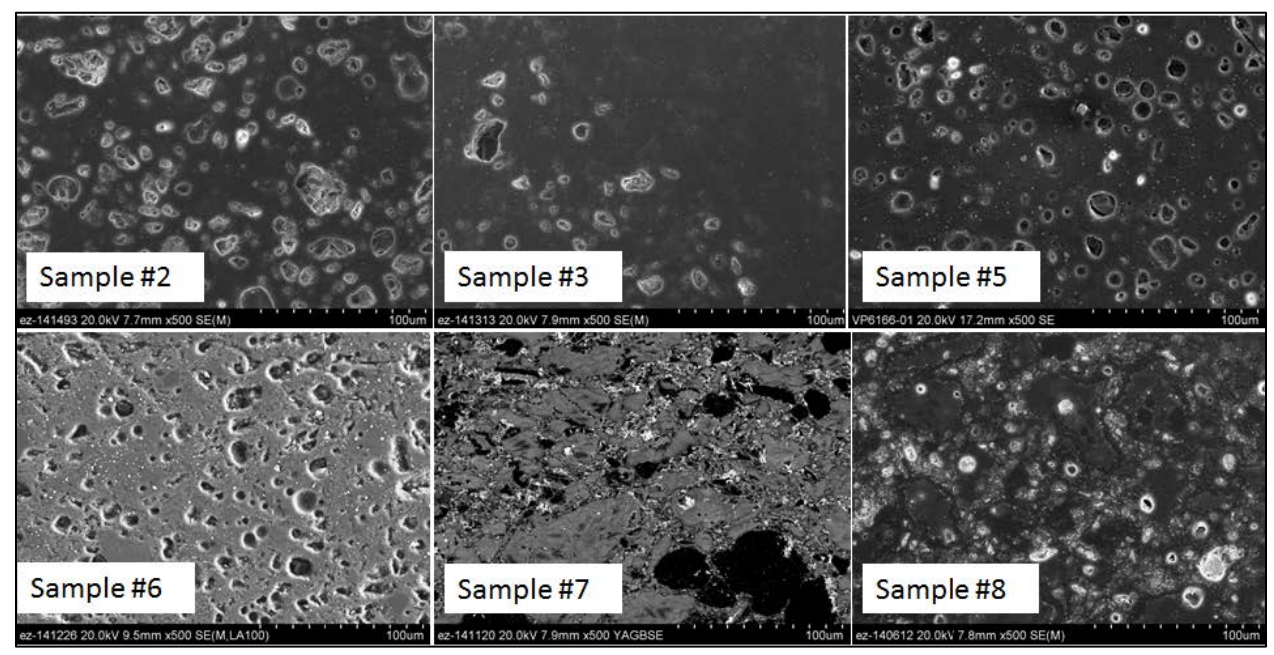


Fig. 20. Sample surfaces 1-2, 1-3, 1-5, 1-6, 1-7, and 1-8 at 500× magnification.

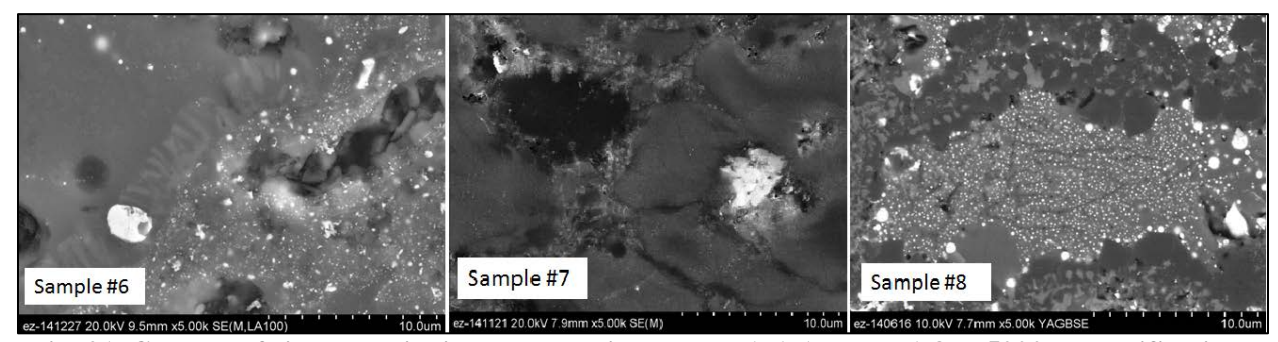


Fig. 21. Clusters of silver and iodine observed in samples 1-6, 1-7, and 1-8 at 5000× magnification.

Elemental maps for sample 1-5 are shown in Fig. 22 and are representative of samples 1-2 through 1-5. The brightness of the color in the map correlates with the concentration of the element being mapped. Elemental maps for samples 1-3 and 1-4 are found in Appendix B. The elemental maps for samples 1-2 through 1-5 do demonstrate some segregation of silicon and the presence of silver clusters. The elemental map for 1-7 is shown in Fig. 23, and the elemental map for sample 1-8 is located in Appendix B. In both 1-7 and 1-8, the silver and iodine present together in clusters and are somewhat homogenously distributed throughout the surface portion investigated.

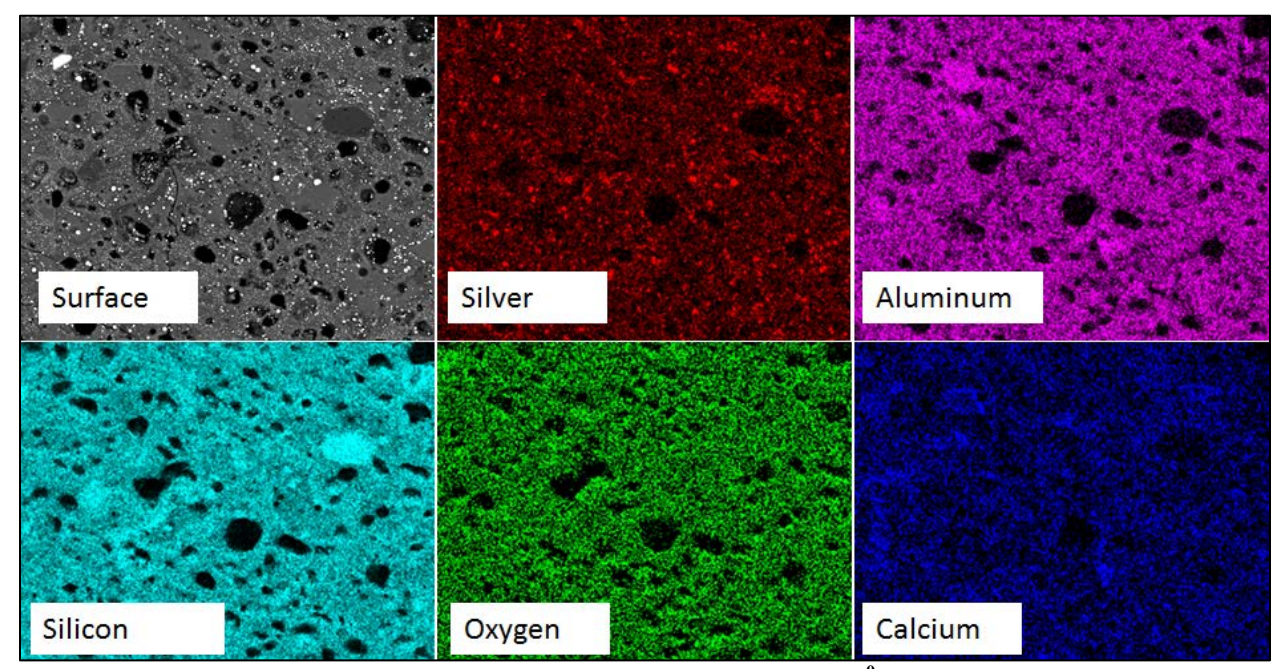


Fig. 22. Elemental maps of HIPed sample surface 1-5 (Ag⁰Z, 850°C, 100 MPa).

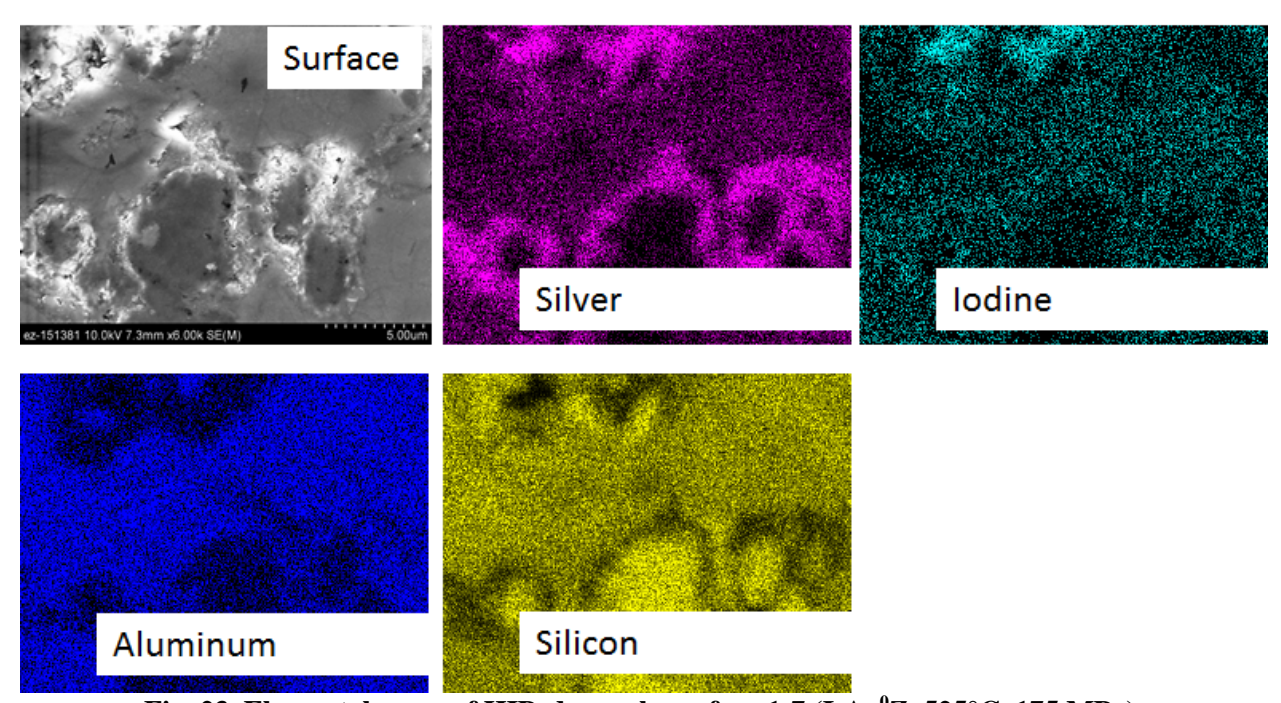


Fig. 23. Elemental maps of HIPed sample surface 1-7 (I-Ag⁰Z, 525°C, 175 MPa).

Finally, energy-dispersive X-ray spectroscopy (EDS) was performed on samples 1-5, 1-7, and 1-8. Sample 1-5 was considered to represent the non-iodine-loaded materials, and both iodine-loaded samples were examined. EDS verified the observations from the elemental maps shown in Fig. 22 of silver clusters and silicon segregation. Figure 24 shows the SEM-EDS spectra of two locations the surface of sample 1-5. The portion of the surface being examined is mapped in the upper left of each spectrum, and the specific point analyzed by EDS is denoted by a red circle. In Fig. 24(a), the spectrum for an observed cluster identifies it as silver, and Fig. 24(b) demonstrates that the area directly adjacent to the cluster is depleted in silver and contains magnesium, aluminum, and silicon. Similar results were observed for

iodine-containing sample 1-7, with the exception that there was some iodine present with the silver clusters. Iodine-containing sample 1-8 (pressed at higher temperature than 1-7) was observed to have more segregation between the amorphous and silver-iodine phases. In Fig. 25 the EDS of sample 1-8 identifies a silver-iodide phase that is clearly separated from the amorphous material around it.

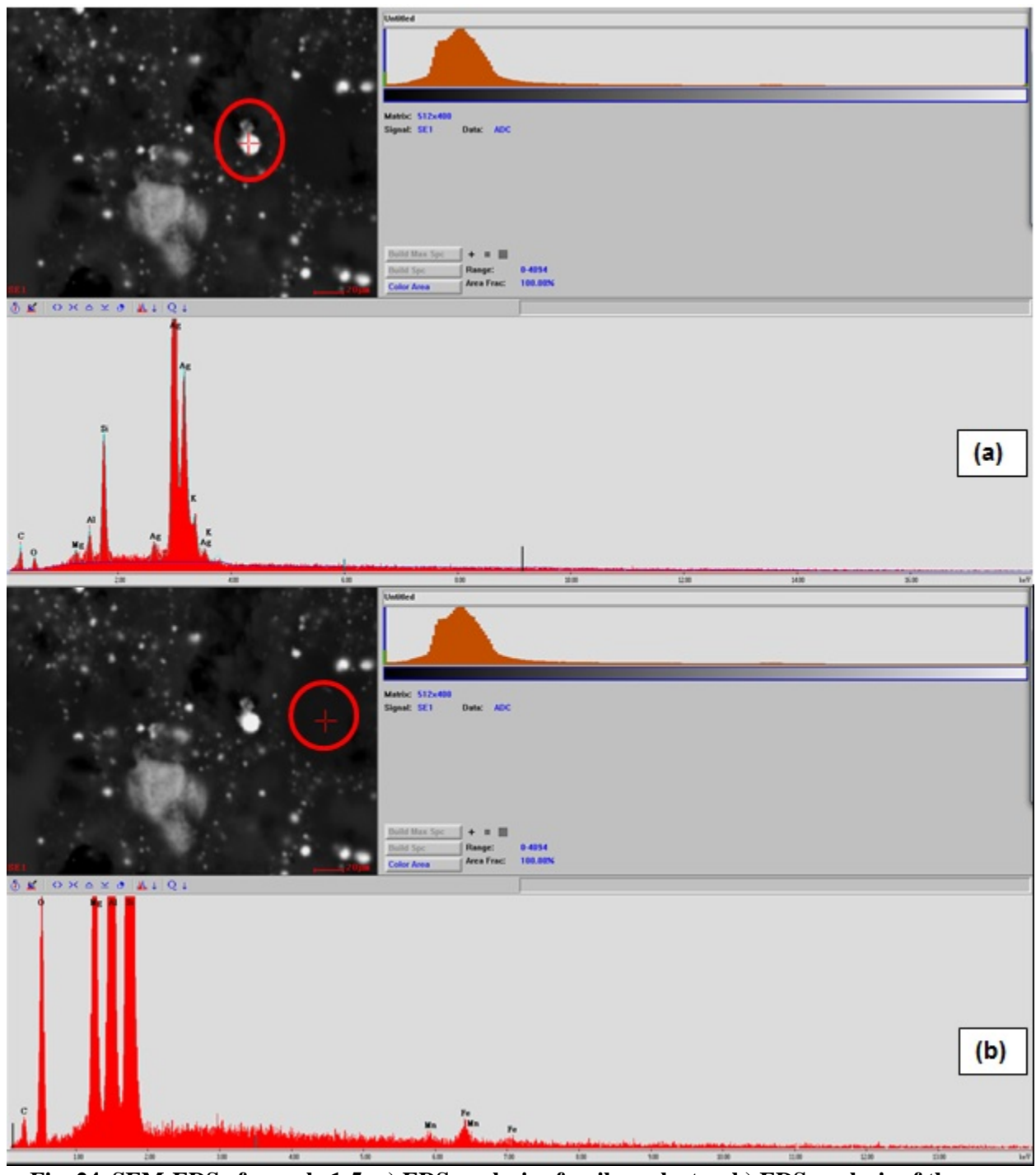


Fig. 24. SEM-EDS of sample 1-5: a) EDS analysis of a silver cluster, b) EDS analysis of the area adjacent to the cluster.

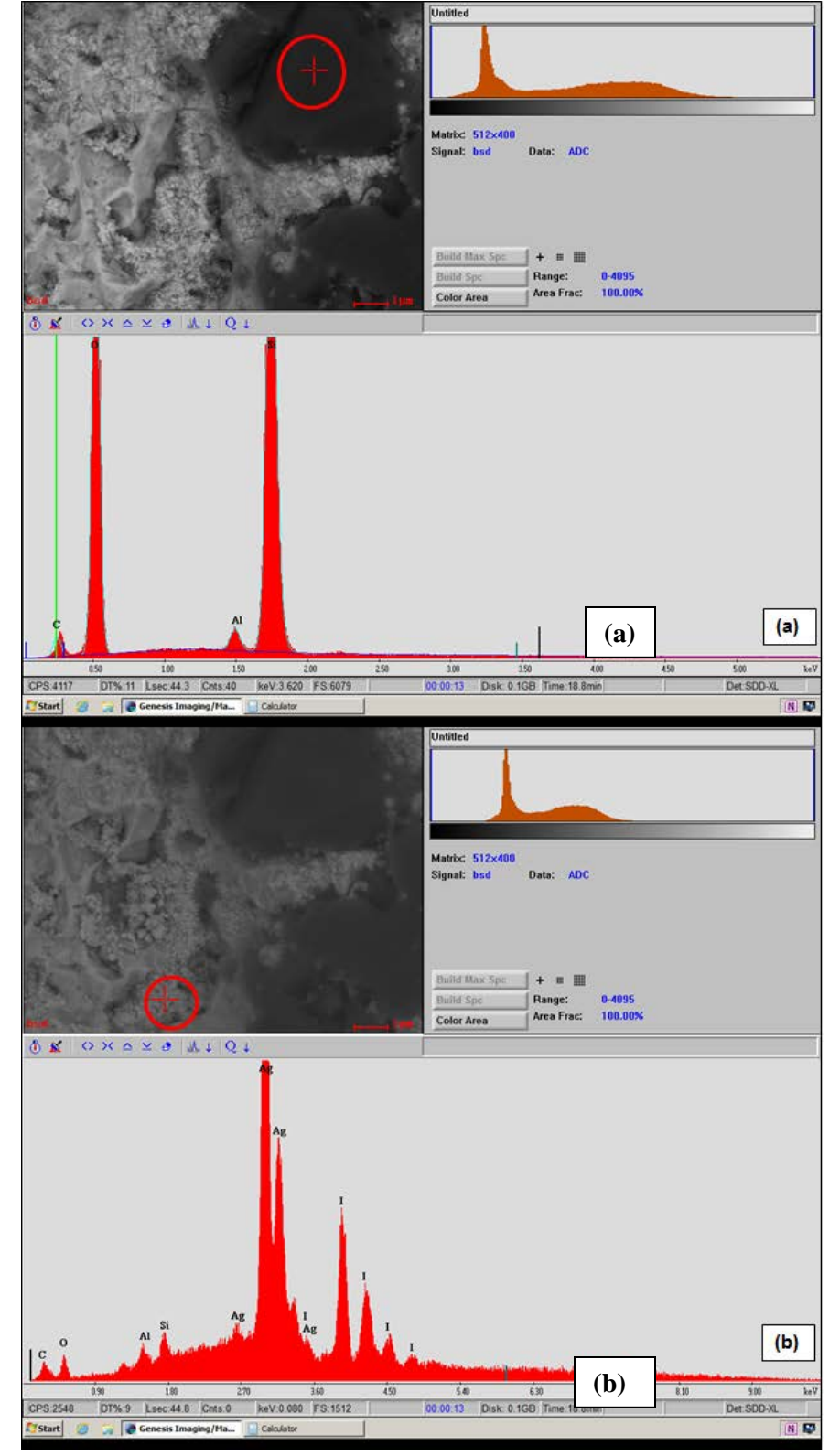


Fig. 25. SEM-EDS of sample 1-8: a) EDS of a silicon structure, b) EDS of AgI clusters observed adjacent to the silicon structure.

5.2 Phase II Pressing and Analysis

5.2.1 Sample Test Matrix

The sample matrix designed for Phase II (Table 5) was more extensive than Phase I and focused on investigating the use of three zeolite materials (sodium zeolite powder, silver zeolite powder, and the engineered silver mordenite used in Phase I) and two forms of iodine (sodium iodide and silver iodide). The parameters studied by use of the test matrix are shown in Table 6.

Table 5. Phase II test matrix

Sample ^{a,b,c}	Temperature (°C)	Pressure (MPa)	Particle form and volume ratio	Notes
2-1	525	175	NaZ Powder + AgI (3:1)	Pure Zeolite
2-2	700	175	NaZ Powder + AgI (3:1)	Pure Zeolite
2-3	900	175	NaZ Powder + AgI (3:1)	Pure Zeolite
2-4 ^a	700	175	NaZ Powder + AgI (6:1)	Pure Zeolite
2-5	900	175	NaZ Powder + AgI (6:1)	Pure Zeolite
2-6	700	300	NaZ Powder + AgI (6:1)	Pure Zeolite
2-7	700	300	NaZ Powder + AgI (3:1)	Pure Zeolite
2-11	900	100	NaZ Powder + AgI (3:1)	Pure Zeolite
2-12	900	175	Ground $Ag^{\circ}Z + AgI(3:1)$	Engineered Zeolite
2-13	900	175	Ground Ag°Z + AgI (6:1)	Engineered Zeolite
2-21	1100	175	NaZ Powder + AgI (3:1)	Pure Zeolite
2-22	1100	175	AgZ Powder + AgI (3:1)	Pure Zeolite
2-23 ^b	900	175	NaZ Powder + NaI (3:1)	Pure Zeolite
2-24	900	175	NaZ Powder + NaI (6:1)	Pure Zeolite

^aSample 2-4 expanded during pressing

^bSample 2-23 did not compress during pressing

^cSamples 2-8, 2-9, 2-10, 2-14 through 2-20 are being investigated in Phase III; not addressed in this report

Tuble 0.1 arameter explored in 1 hase it testing							
Set	Samples	Primary effect studied	Secondary effect				
1	1, 2, 3	HIP temperature					
2	2, 4 ^a	NaZ / AgI ratio	HIP temperature				
3	3, 5	NaZ / AgI ratio	HIP temperature				
4	2, 6	Pressure	NaZ / AgI ratio				
5	4, ^a 7	Pressure	NaZ / AgI ratio				
11	21,22 ^c	AgZ vs NaZ	HIP temperature				
12	11, 3	Pressure	Also compare to sample 7				
13	12, 13	Zeolon / AgI ratio					
14	13, 9 ^c	Zeolon / Pure					
15	12, 8 ^c	Zeolon / Pure					
16	23, ^b 24	NaZ / NaI ratio	Iodine scrubber waste				
17	23, 5 3	NaI vs AgI					
18	24, 5	NaI vs AgI					

Table 6. Parameter explored in Phase II testing

The pressed samples are similar in capsule appearance to samples created in Phase I. The cross sections of samples 2-12 and 2-13 are relatively uniform in appearance; these are the two samples with engineered silver zeolite as the primary component. Sample 2-13 is shown in Fig. 26. Samples 2-2, 2-5, 2-6, 2-7, and 2-11 all contained sodium zeolite powder as the primary component, with iodine added in the form of AgI. The cross section of each of these samples varied significantly in appearance. Sample 2-7 is shown as an example (Fig. 27), and samples 2-2, 2-5, and 2-6 are found in Appendix A. Sample 2-11, pressed at the lowest pressure of 100 MPa, was found to have a number of voids upon cross sectioning (Fig. 28). These voids reflect gas pocket formation, but it is unknown what type of gas was present.



Fig. 26. Cross section of sample 2-13 (engineered Ag⁰Z + AgI 3:1; 900°C and 100 MPa).

^aSample 2-4 expanded during pressing

^bSample 2-23 did not compress during pressing

^cSamples 2-8, 2-9, and 2-22 investigated in Phase III; not addressed in this report



Fig. 27. Cross section of sample 2-7 (NaZ + AgI 3:1; 700°C and 300 MPa).



Fig. 28. Cross section of sample 2-11 (NaZ + AgI 3:1; 900°C and 100 MPa).

5.2.2 Analysis of Phase II Samples

The density of the resulting product in the pressed samples was determined by volume displacement, as in Phase I. Table 7 shows the resulting densities of the HIPed samples. The density measurements do not clearly correlate with pressing conditions or sample composition. Set 1, identified in Table 6, shows a density increase with increased pressing temperature. There is some indication from Set 12 that increased pressure results in increased density, but this is not supported by the results from Set 4. As a stand-alone measurement, variations in density of the pressed pellets are not an indication of an ideal sample

composition. However, when taken in concert with other analyses such as XRD and SEM-EDS, it may help identify a best sample composition.

Table 7. Density of HIPed Phase II samples

Sample	Temperature (°C)	Pressure (MPa)	Time (hr)	Particle form	Weight (g)	Avg. density (g/cc)	Std dev of Density
2-1	525	175	3	NaZ Powder + AgI (3:1)	10.9391	1.738	0.000
2-2	700	175	3	NaZ Powder + AgI (3:1)	10.9801	2.046	0.531
2-3	900	175	3	NaZ Powder + AgI (3:1)	11.023	1.743	0.000
2-4 ^a	700	175	3	NaZ Powder + AgI (6:1)	10.6806	0.302	0.024
2-5	900	175	3	NaZ Powder + AgI (6:1)	10.8683	1.187	0.000
2-6	700	300	3	NaZ Powder + AgI (6:1)	10.8891	2.173	0.497
2-7	700	300	3	NaZ Powder + AgI (3:1)	10.9183	2.196	0.782
2-11	900	100	3	NaZ Powder + AgI (3:1)	10.9364	1.027	0.000
2-12	900	175	3	Ground Ag°Z + AgI (3:1)	14.3215	2.870	0.359
2-13	900	175	3	Ground Ag°Z + AgI (6:1)	14.4158	2.604	0.359
2-21	1100	175	3	NaZ Powder + AgI (3:1)	10.5457	2.516	0.000
2-23 ^b	900	175	3	NaZ Powder + NaI (3:1)	11.0469	0.460	0.023
2-24	900	175	3	NaZ Powder + NaI (6:1)	10.8111	2.166	0.491

^aSample 2-4 expanded during pressing

XRD was performed on all Phase II samples with the exception of 2-4 and 2-23, which were not pressed successfully. Samples 2-5 and 2-24 had a cross section that was too small to be analyzed, and the resulting spectra showed only the stainless steel container. All other samples were primarily amorphous and showed only three distinct compounds: AgI in the form of miersite and or iodargyrite, elemental silver, and SiO₂. The diffraction patterns for samples 2-1, 2-2, and 2-3 are shown in Fig. 29, and the patterns for each of the other Phase II samples can be found in Appendix C.

^bSample 2-23 did not compress during pressing

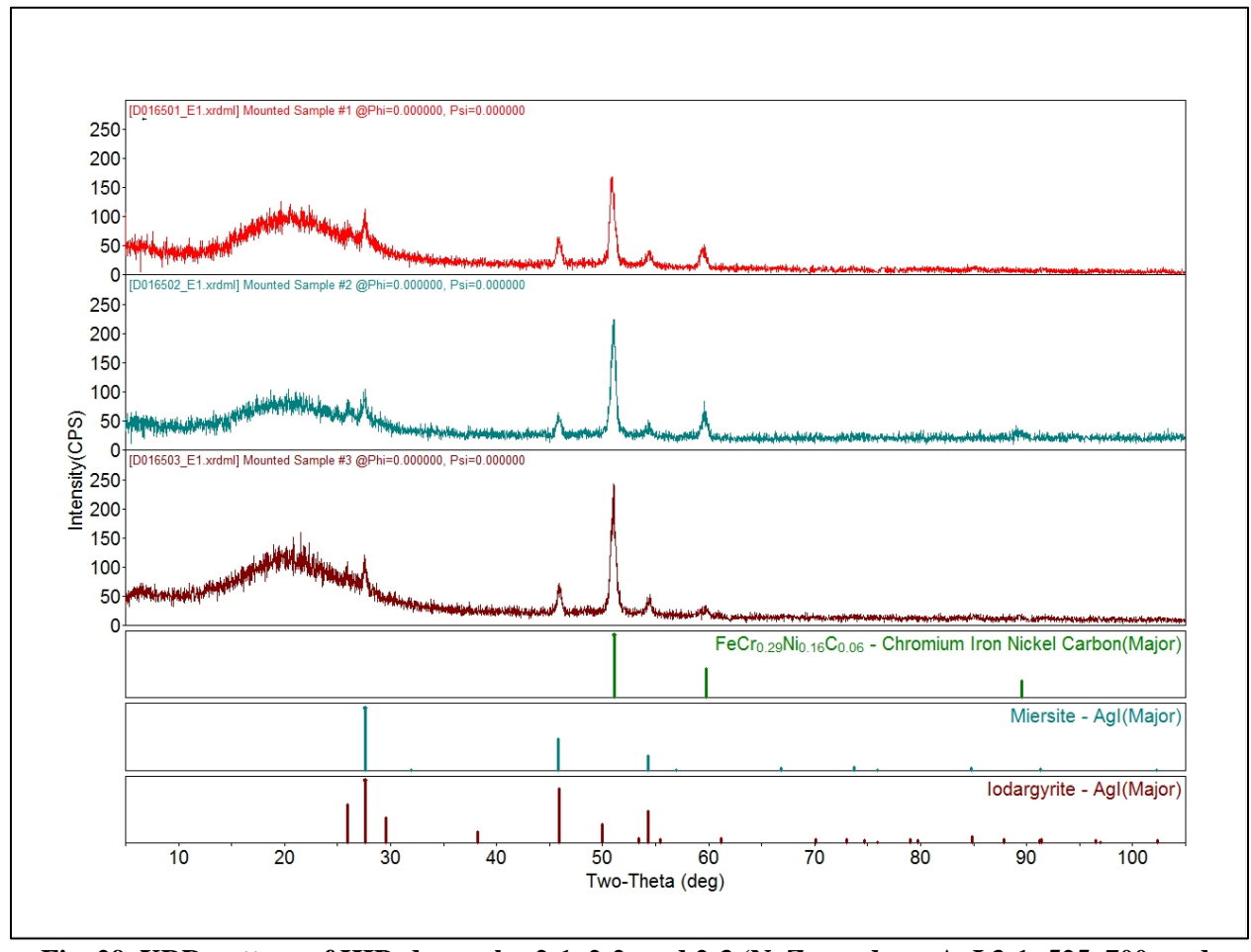


Fig. 29. XRD pattern of HIPed samples 2-1, 2-2, and 2-3 (NaZ powder + AgI 3:1; 525, 700, and 900° C, respectively).

As in Phase I, the surface of each sample was analyzed using SEM-EDS. At low magnification, pitting was again observed (Fig. 30), along with the presence of AgI clusters. The cause of the pitting is currently unknown. In samples 2-2 and 2-6, these AgI clusters are quite large but are smaller and homogenously distributed on the portion of the surface examined for samples 2-7 and 2-24. Variations in pressing conditions and sample composition do not explain this difference.

Sample 2-13, a sample containing engineered Ag^0Z , displays an occluded crystalline structure when examined at higher magnifications (Fig. 31). As the XRD patterns did not indicate any other mineral phases other than AgI and SiO_2 , this structure may be quartz. The XRD pattern for sample 2-13 is found in Appendix C.

The elemental maps obtained for Phase II samples do not vary significantly with pressing conditions and sample composition. A representative set of maps is shown in Fig. 32 of the surface of sample 2-1. Maps for 2-7, 2-11, and 2-12 are found in Appendix B. In each sample, silver and iodine are located in clusters together and distributed homogenously across the portion of the sample surface under examination. The EDS spectra correlate with this observation and indicate that AgI is not incorporated into siliconcontaining phases. This shows that production of a known iodine-containing mineral, as would be desirable, has not occurred. Representative EDS is shown for sample 2-3 in Fig. 33.

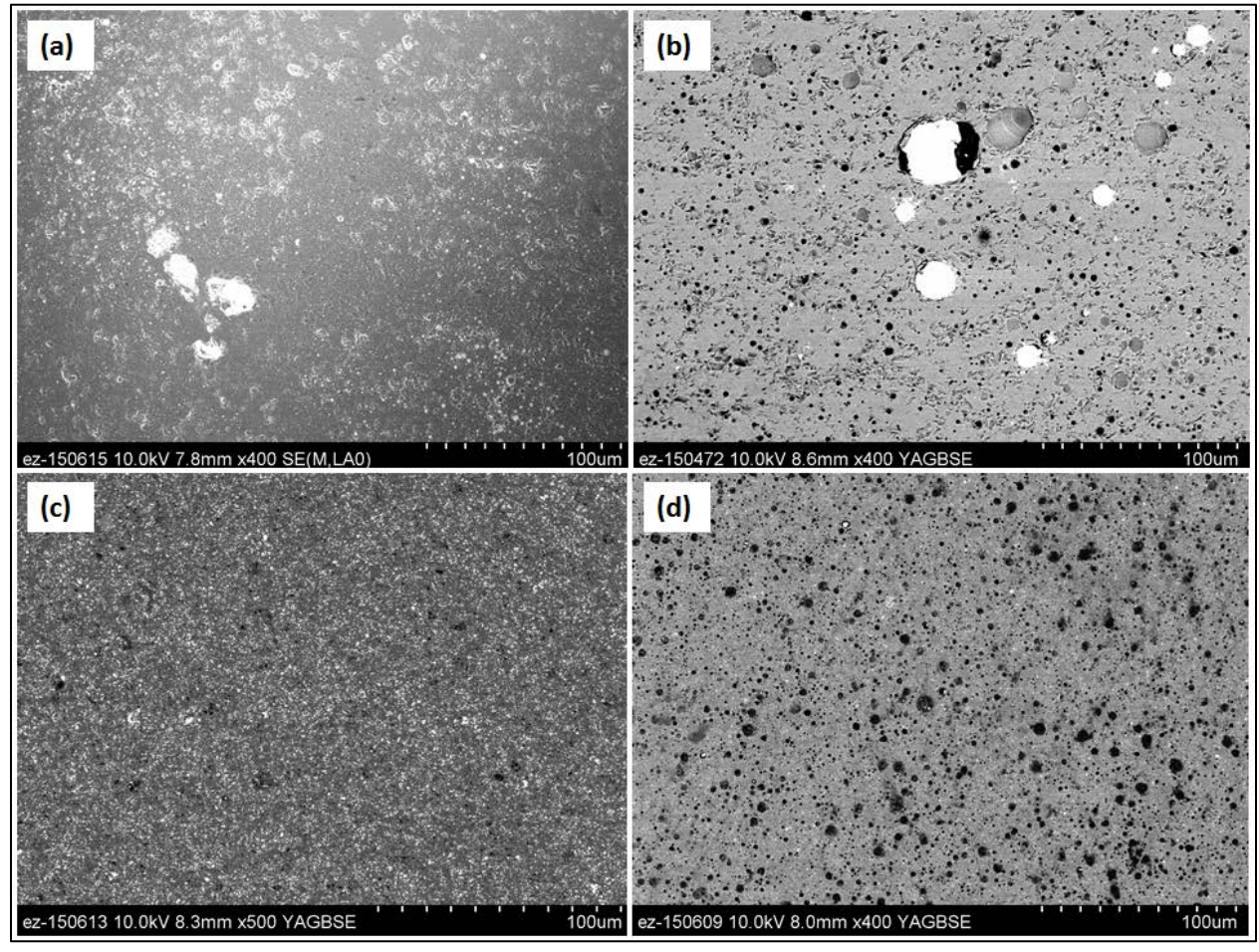


Fig. 30. Surfaces of sample 2-2 (a), sample 2-6 (b), sample 2-7 (c), and sample 2-24 (d) at $400 \times$ magnification (pressing conditions and sample compositions found in Table 7).

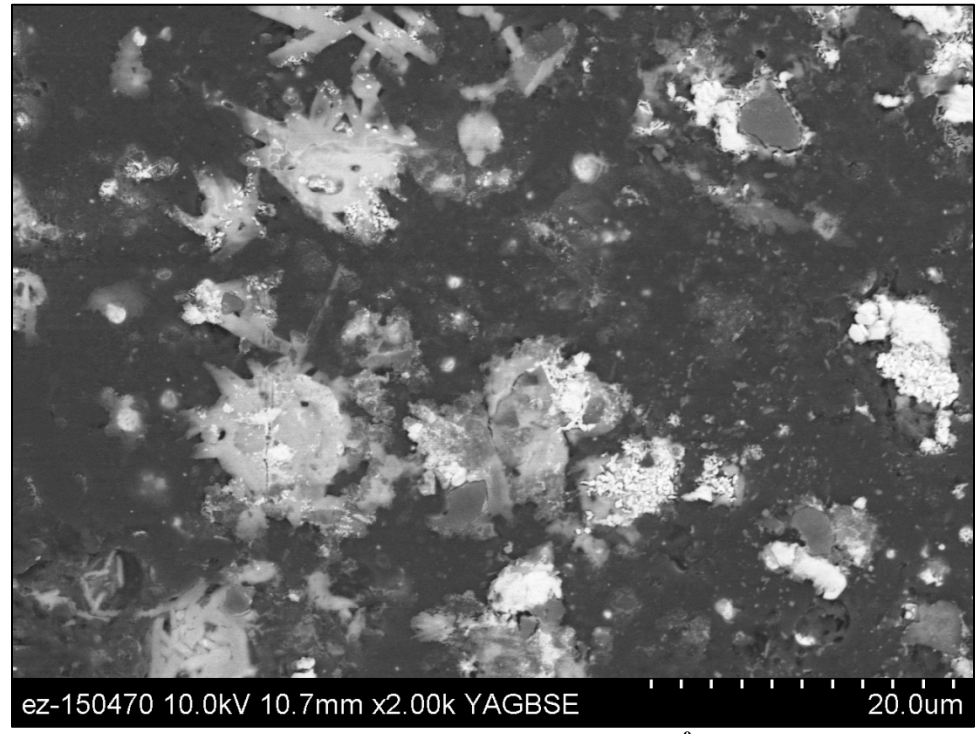
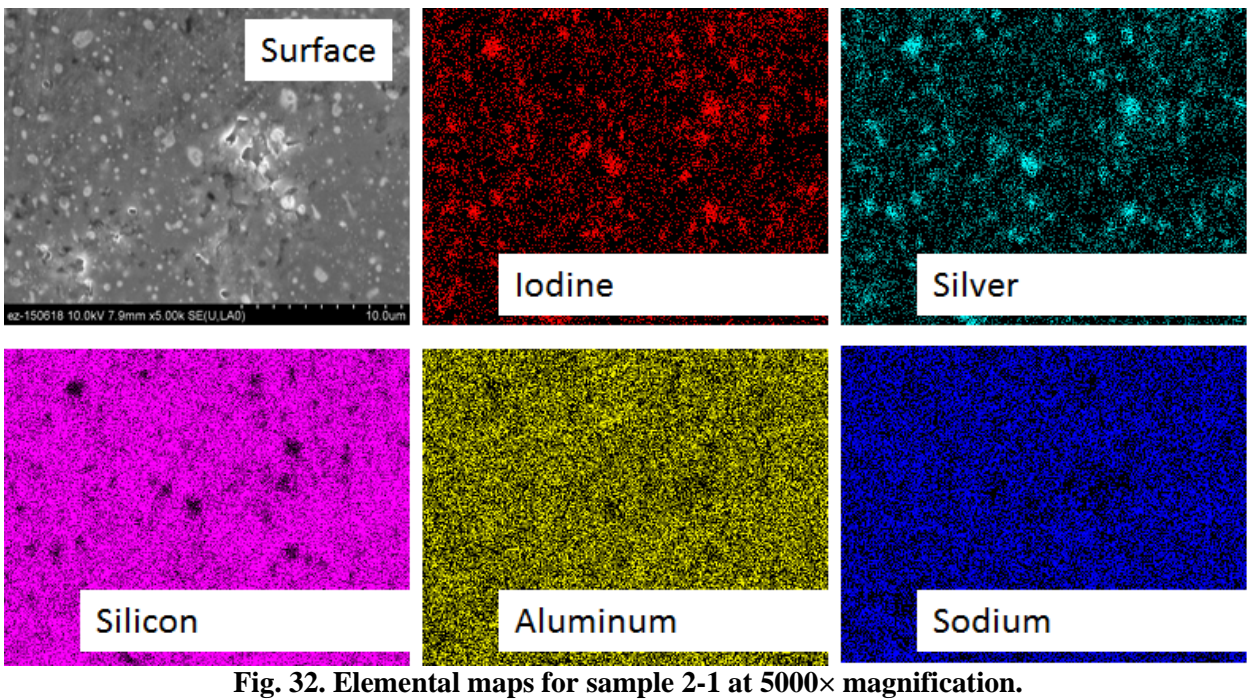


Fig. 31. Surface of sample 2-13 (containing engineered Ag⁰Z) at 2000× magnification.



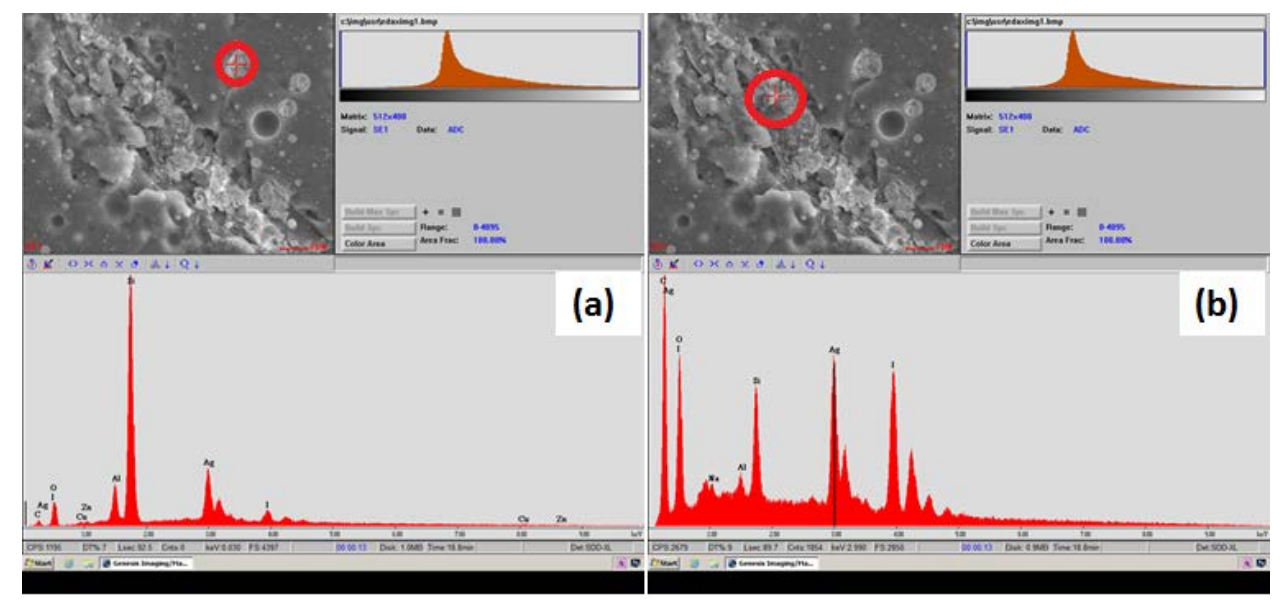


Fig. 33. SEM-EDS of sample 2-3: a) EDS of a silicon structure, b) EDS of AgI clusters observed adjacent to the silicon structure.

DISCUSSION 6.

The purpose of this study was to determine if hot pressing could directly convert iodine-loaded silverexchange mordenite (I-Ag⁰Z) into a suitable waste form. Initial scoping studies utilized HUPing to prepare pressed samples of AgZ. While resulting pellets did have an increase in density of 70% over the starting material, the samples were not found to be durable when subjected to a crush test. The use of HIPing was suggested as a way to produce a waste form with increased robustness.

HIPing was carried out in two phases, and a third is under way. Phase I evaluated the effects of pressure and temperature conditions on the manufacture of a pressed sample from Ag⁰Z and I-Ag⁰Z. It was found that HIPing resulted in a pressed pellet with a density over 300% of the starting material, and the pellet was very mechanically stable. To determine whether the pressing conditions resulted in a transformation of the material from mordenite into another iodine-containing mineral phase, each pressed pellet was analyzed by SEM-EDS and XRD. It was shown that under the conditions used for pressing, the majority of the material transforms into an amorphous structure. The only crystalline phase observed in the pressed Ag⁰Z material was SiO₂. For the samples loaded with iodine (I-Ag⁰Z), iodine was present as AgI clusters at low temperatures and transformed into AgIO₄ at high temperatures. Surface mapping and EDS demonstrate segregation between silver iodide phases and silicon dioxide phases, further supporting the lack of a mineral-phase formation.

Based on the results of the Phase I study, an expanded test matrix was developed to examine the effects of multiple source materials, compositional variations, and an expanded temperature range. Each sample was analyzed with the sample approach used in Phase I. In all cases, there is nothing in the SEM or XRD analyses that indicates creation of any AgI-containing silicon phase, with the samples being found to be largely amorphous. Phase III of this study has been initiated. It will build upon the information gathered in Phase II and will examine the durability of the pressed pellet through product consistency testing (PCT) studies. If the pellet is found to have high iodine retention, the lack of crystalline structure identified through the work described in this report may not be considered to be concerning for long-term stability and disposition. Upon the conclusion of the Phase III study, a report will be issued that will

summarize the experimental work completed in all three phases and will provide recommendations as to the promise of HIPing for the production of an iodine-containing waste pellet.

7. REFERENCES

- 1. A. B. CHRISTENSEN, J. A. DEL DEBBIO, D. A. KNECHT, J. E. TANNER, and S. C. COSSEL, "Immobilization of krypton 85 in zeolite5A," *Proceedings of the 17th DOE Nuclear Air Cleaning Conference*, CONF-820833, pp. 183–197, 1983.
- 2. C. PEREIRA, M. HASH, M. LEWIS, and M. RICHMANN, "Ceramic-Composite Waste Forms from the Electrometallurgical Treatment of Spent Nuclear Fuel," *Journal of Materials*, 34–40, July 1997.
- 3. STEPHEN PRIEBE and KEN BATEMAN, "The Ceramic Waste Form Process at Idaho National Laboratory," *Nuclear Technology*, 199, 207 (162), May 2008.
- 4. EWAN MADDRELL, "Capture and Immobilization of Iodine," National Nuclear Laboratory, November 2, 2005.
- 5. TSUTOMU NISHIMURA, TOMOFUMI SAKURAGI, YUJI NASU, HIDEKAZU ASANO, and HIROMI TANABE, "Development of immobilization techniques of radioactive iodine for geological disposal," Mobile Fission and Activation Products in Nuclear Waste Disposal, January 16–19, 2007, mofap07.in2p3.fr/17janvier/Mofap07%20OHP%20T.pdf
- 6. PECHAR, F., and D. RKYL, "Thermal Decomposition of Natural Mordenite," *Chem Papers*, 41(3), 351–362, 1987.

Appendix A

Cross Sections of Phase I and II Samples



Fig. A-1. Cross section of sample 1-5 (850°C, 100 MPa).



Fig. A-2. Cross section of sample 1-7 (525°C, 175 MPa).



Fig. A-3. Cross section of sample 2-2 (700° C, 175 MPa).



Fig. A-4. Cross section of sample 2-5 (900°C, 175 MPa).

Fig. A-5. Cross section of sample 2-6 (700°C, 300 MPa).



Fig. A-6. Cross section of sample 2-13 (900° C, 175 MPa).

Appendix B

Elemental Maps of Pressed Samples

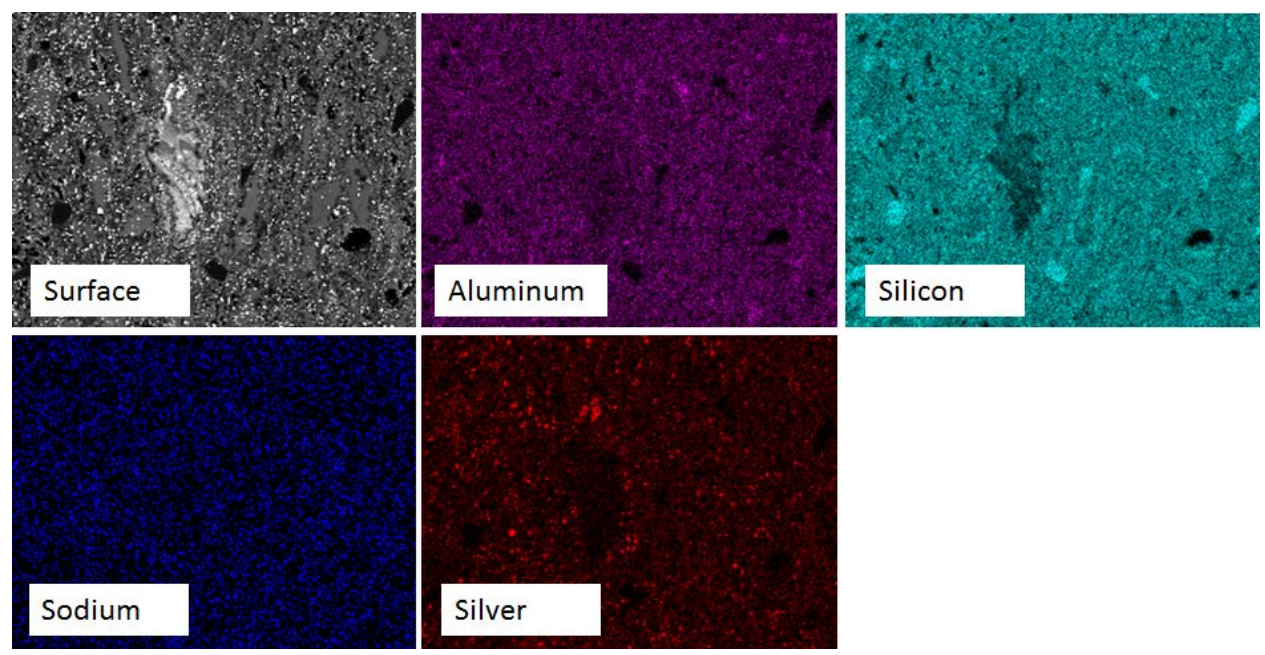


Fig. B-1. Elemental maps for sample 2-1 at ≈500× magnification.

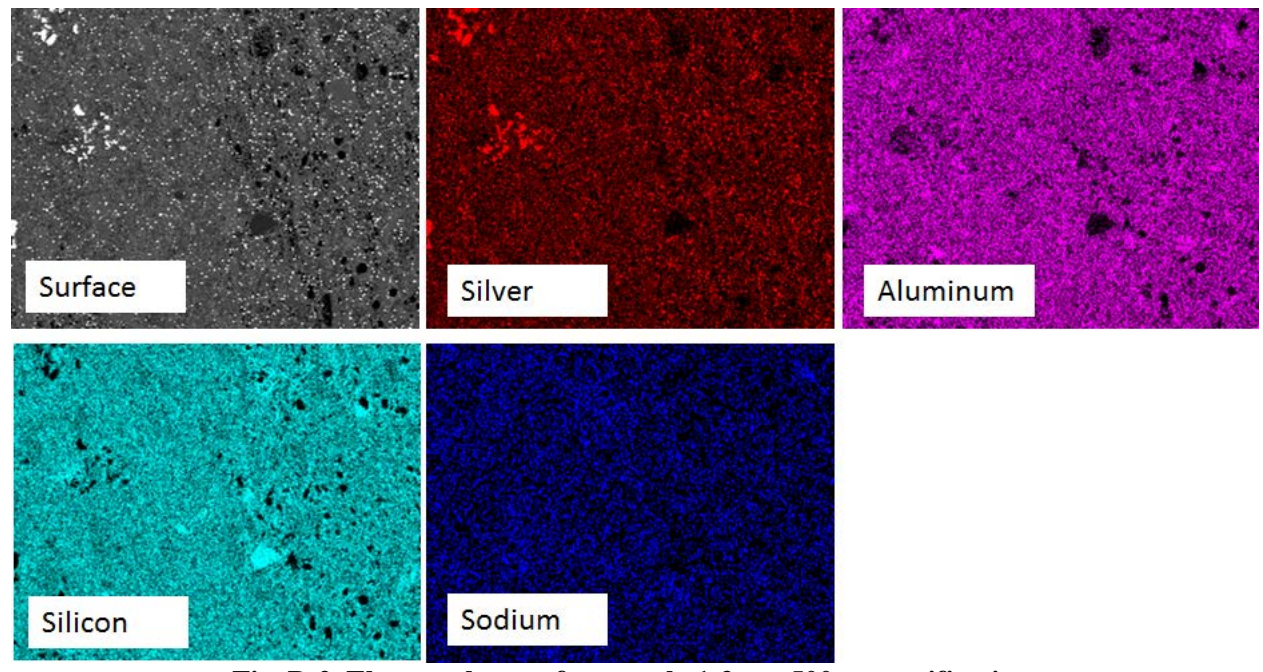


Fig. B-2. Elemental maps for sample 1-3 at \approx 500× magnification.

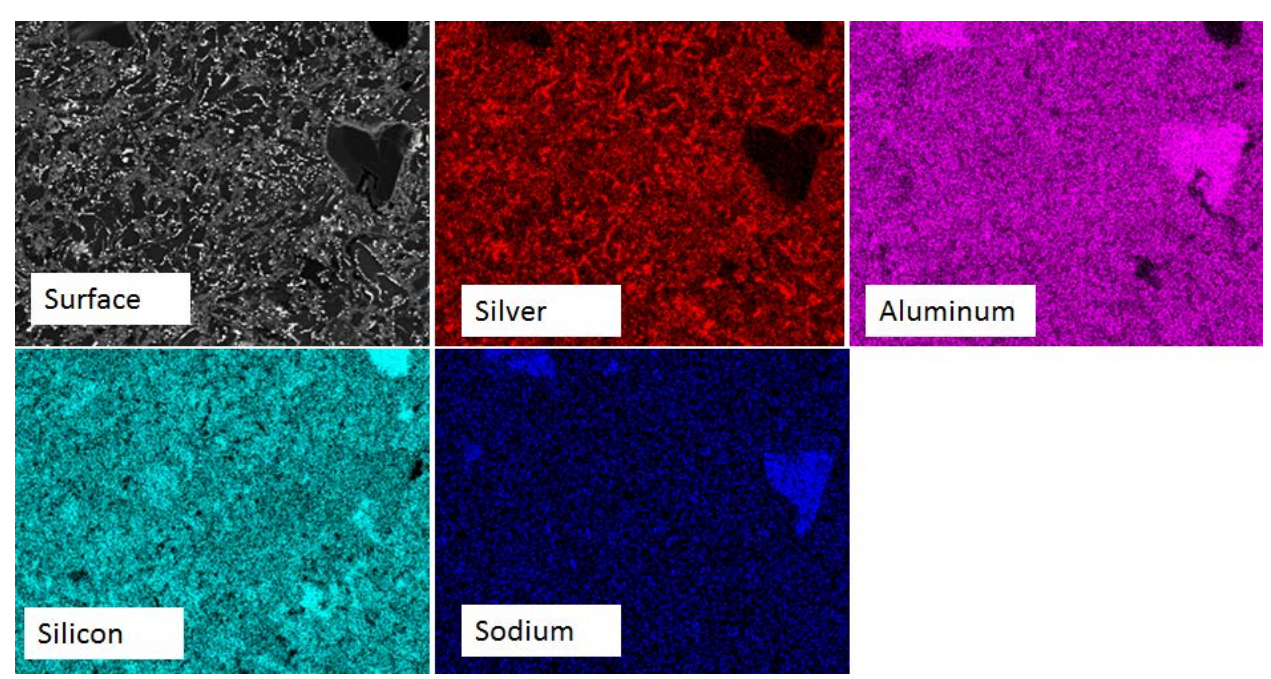


Fig. B-3. Elemental maps for sample 1-4 at ≈500× magnification.

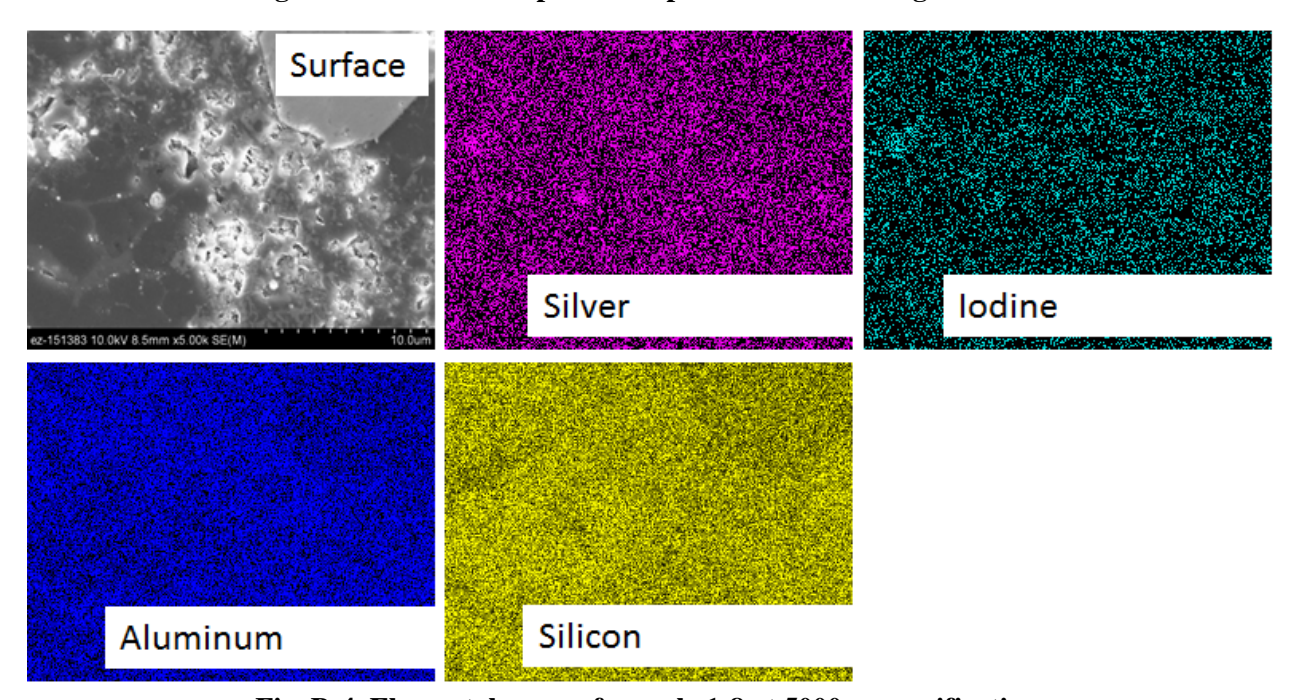


Fig. B-4. Elemental maps of sample 1-8 at $5000 \times$ magnification.

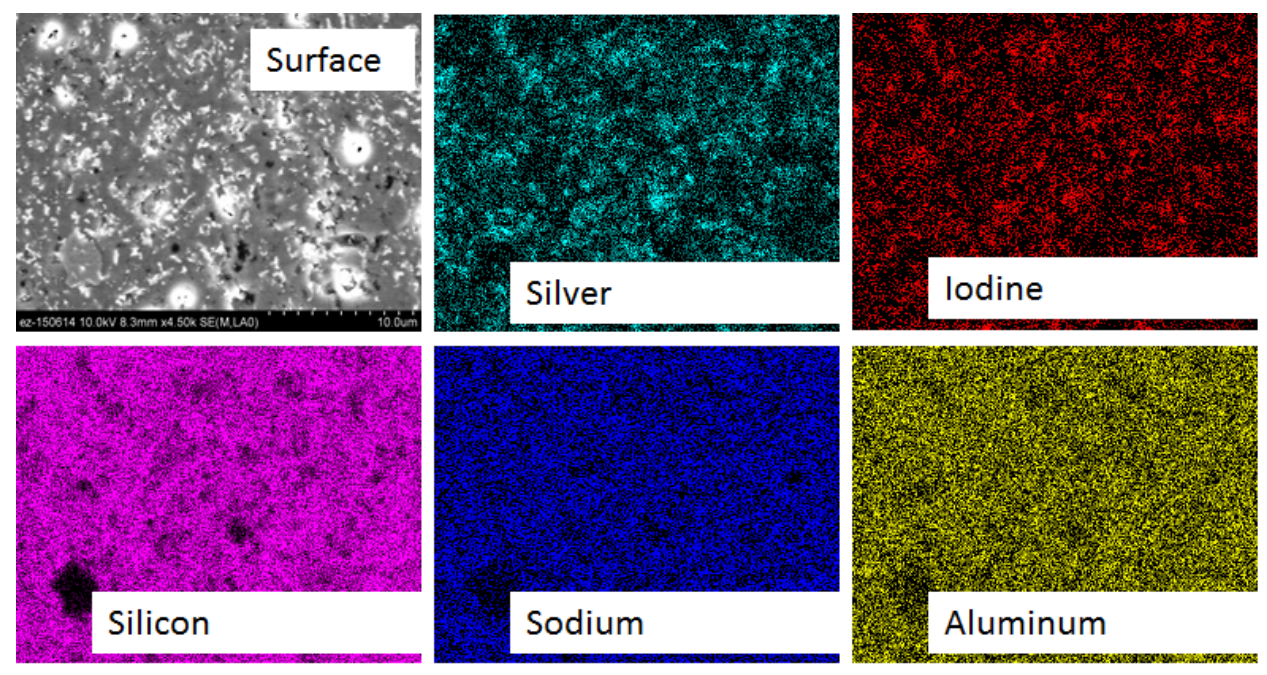


Fig. B-5. Elemental maps of sample 2-7 at 50000× magnification.

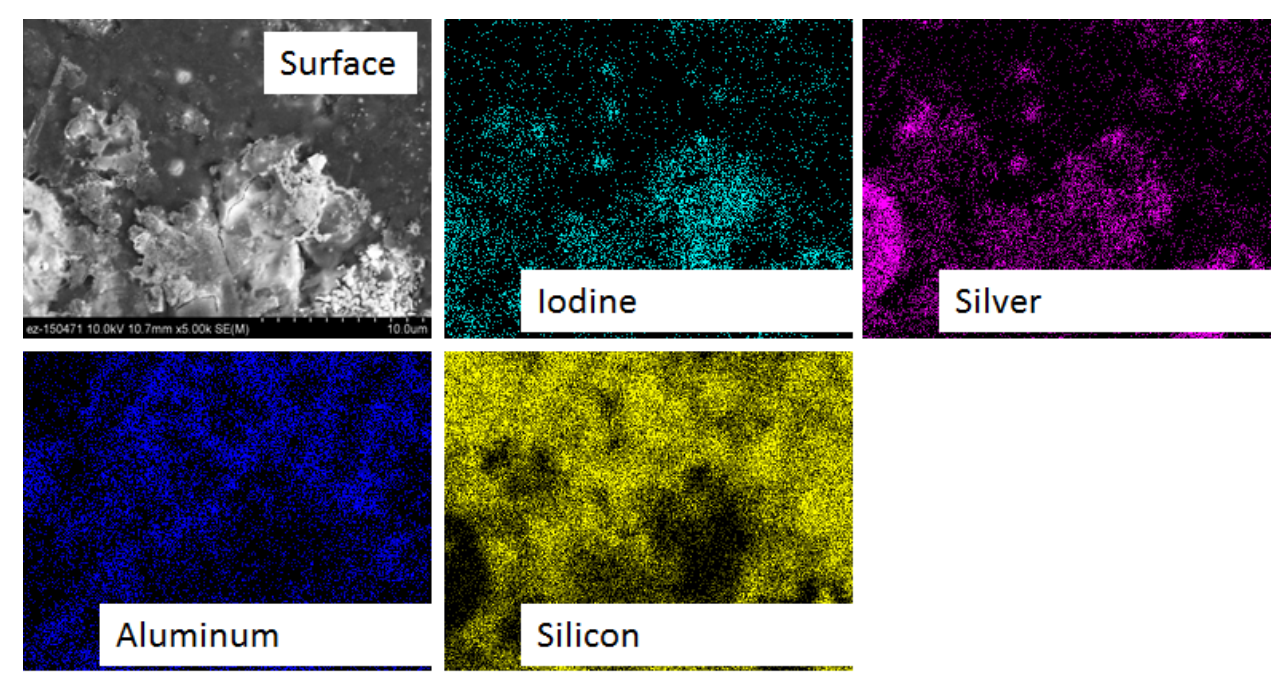
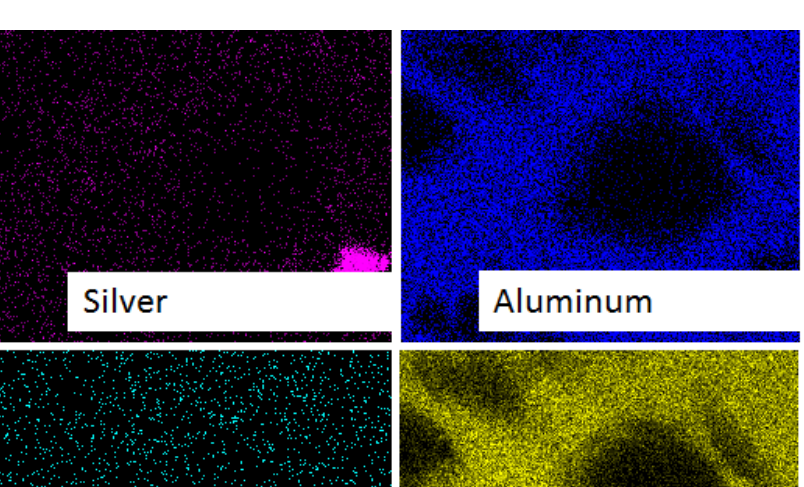


Fig. B-6. Elemental maps of sample 2-11 at $5000 \times$ magnification.

Surface



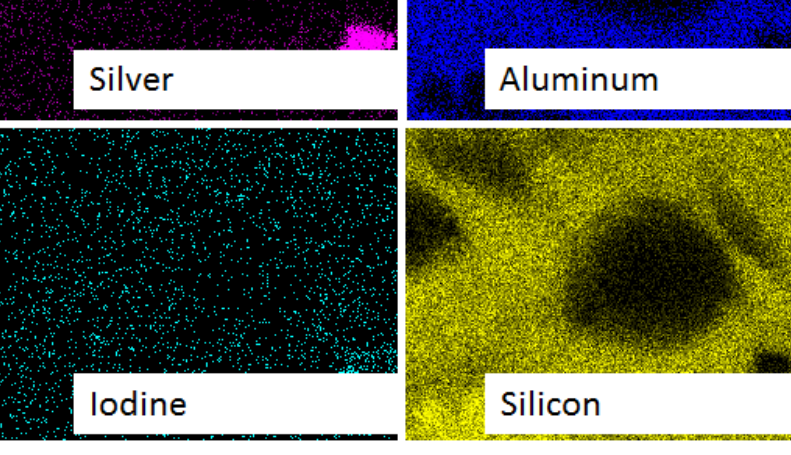


Fig. B-7. Elemental maps of sample 2-12 at $5000 \times$ magnification.

Appendix C

XRD Patterns of Phase II Samples

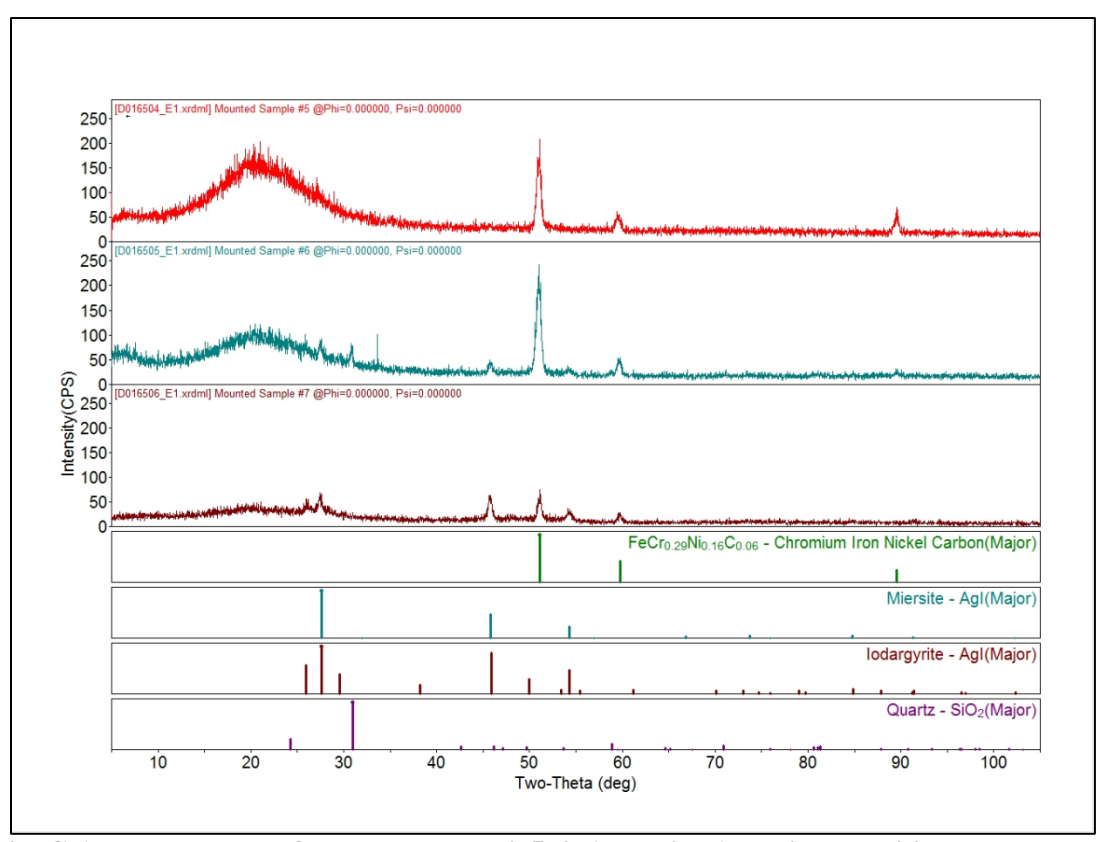


Fig. C-1. XRD pattern of HIPed samples 2-5, 2-6, and 2-7 (pressing conditions and sample composition found in Table 7).

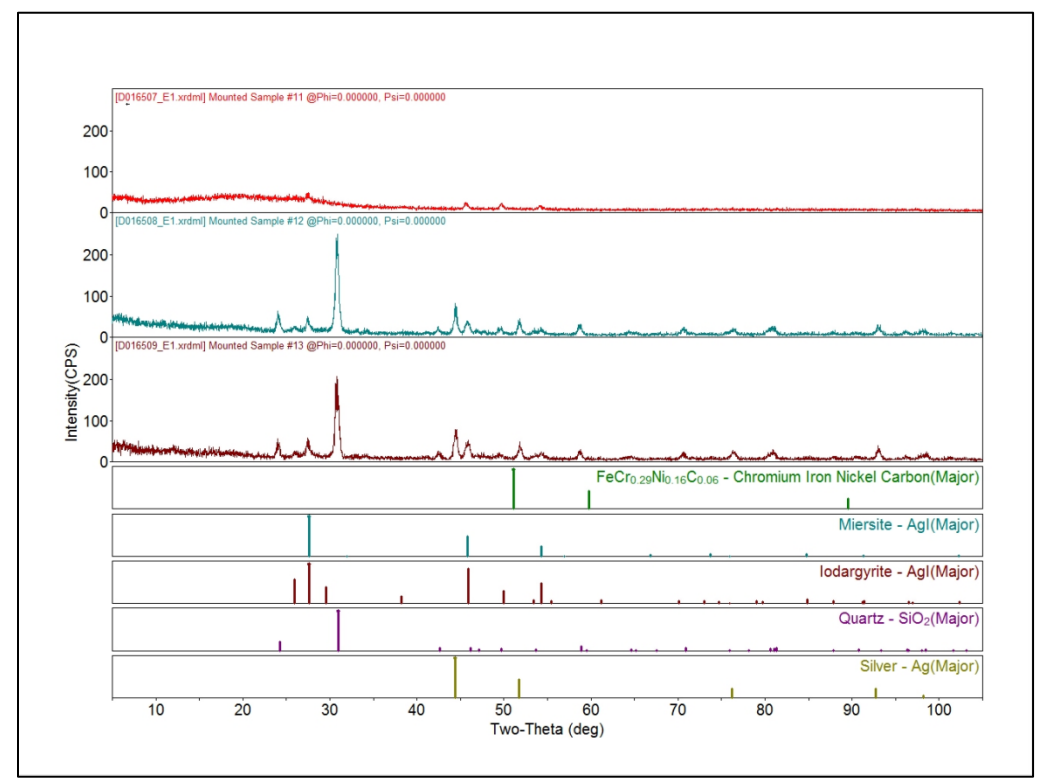


Fig. C-2. XRD pattern of HIPed samples 2-11, 2-12, and 2-13 (pressing conditions and sample composition found in Table 7).

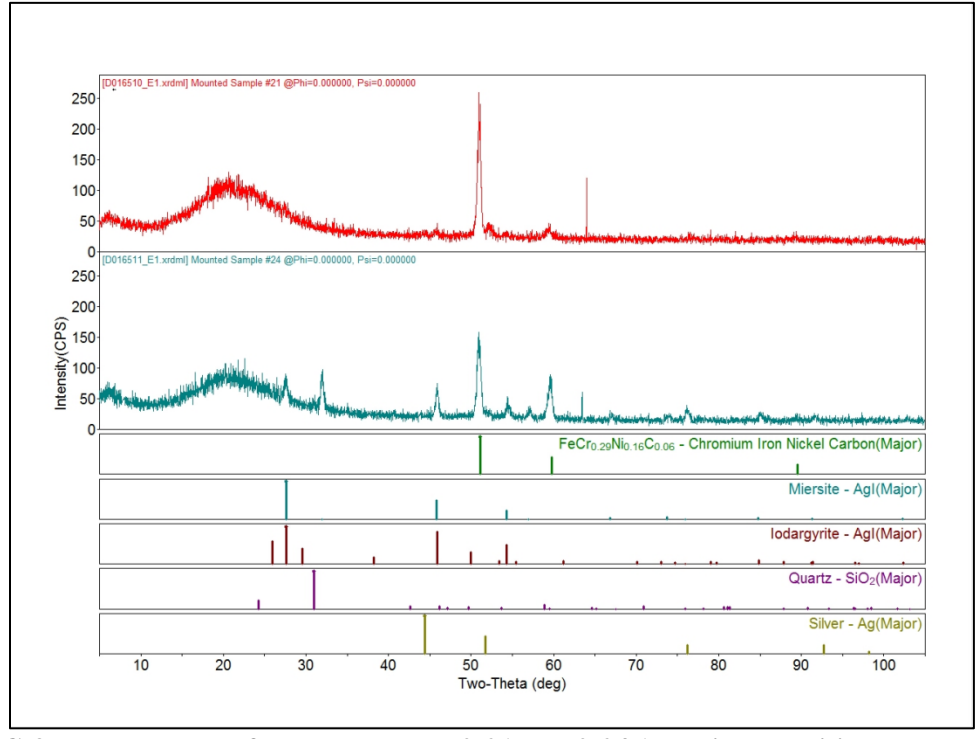


Fig. C-3. XRD pattern of HIPed samples 2-21 and 2-24 (pressing conditions and sample composition found in Table 7).